

Performance Analysis of Space-Time Coded Modulation Techniques using GBSB-MIMO Channel Models

Ravikiran Nory

Thesis submitted to the faculty of the
Virginia Polytechnic Institute and State University
in partial fulfillment of the requirements for the degree of

Master of Science
in
Electrical Engineering

Brian D. Woerner, Chair
Jeffrey H. Reed
Charles W. Bostian

June 04, 2002
Blacksburg, Virginia

Keywords: MIMO channels, GBSB channel models, Space Time Block
Coding, Multilayered Space-Time Coding, Wireless Communication.

Copyright 2002, Ravikiran Nory

© Copyright 2002

by

Ravikiran Nory

Performance Analysis of Space-Time Coded Modulation Techniques using GBSB-MIMO Channel Models

by

Ravikiran Nory

Committee Chairman: Dr. Brian D. Woerner

Abstract

Wireless systems are rapidly developing to provide high speed voice, text and multimedia messaging services which were traditionally offered by wire line networks. To support these services, channels with large capacities are required. Information theoretic investigations have shown that Multiple Input Multiple Output (MIMO) channels can achieve very high capacities. Space-Time Block Coding (STBC) and Bell Labs Layered Space-Time Architecture (BLAST) are two potential schemes which utilize the diversity offered by MIMO channels to provide reliable high data rate wireless communication. This work studies the sensitivity of these two schemes to spatial correlation in MIMO channels.

The first part of the thesis studies the effect of spatial correlation on the performance of STBC by using Geometrically Based Single Bounce MIMO (GBSB-MIMO) channel models. Performance is analyzed for two scenarios: one without scatterers in the vicinity of the transmitter and other with scatterers. In the second part of the thesis, the sensitivity of BLAST to spatial correlation is analyzed. Later, schemes which use the principles of Multilayered Space-Time Coded Modulation to combine the benefits of BLAST and STBC are introduced and their performance is investigated in correlated and uncorrelated Rayleigh fading. Results indicate that schemes using orthogonal design space-time block codes are reasonably robust to spatial correlation while schemes like BLAST are very sensitive as they depend on array processing to separate signals from various transmit antennas.

Acknowledgements

Dr. Brian Woerner has been a constant source of advice and encouragement right from the very beginning of my MS program at Virginia Tech. I would like to express my heartfelt gratitude to him. I consider myself extremely fortunate for having him as my advisor. I am grateful to Dr. Jeff Reed and Dr. Charles Bostian for agreeing to be on my thesis committee and reviewing my research work. Special thanks to Dr. Ran Gozali and Dr. Mike Buehrer for their helpful suggestions and insightful comments on my work.

I would like to thank Yasir, Pierre and Venkat for the numerous ‘technical’ discussions I had with them. I would also like to thank the MPRG staff for their outstanding support. Finally, I would like to thank all my colleagues at MPRG and for making my graduate study at Virginia Tech a pleasant experience.

Contents

1. Overview and Contributions	1
1.1 Overview	1
1.2 Outline of Contents	2
1.3 Contributions	3
2. Introduction to Space-Time Block Codes	5
2.1 Multiple Input Multiple Output (MIMO) channels	5
2.2 Fundamentals of Space-Time Block Coding (STBC)	9
2.2.1 Introduction to Transmit Diversity schemes	9
2.2.2 Encoding and Decoding of Space-Time Block Codes	11
2.2.3 Performance of Space-Time Block Coding	14
2.3 Transmit Diversity techniques for 3G wireless systems	17
2.4 Summary	18
3. Performance of STBC in Geometrically Based Channel Models	19
3.1 Introduction to Geometrically Based Single Bounce (GBSB) models	20
3.2 GBSB circular model for MIMO systems	23
3.3 GBSB elliptical model for MIMO systems	32
3.4 Performance analysis of STBC in GBSB models	40
3.4.1 Performance of STBC in circular model	41
3.4.2 Performance of STBC in elliptical model	44
3.4.3 Comparison of results with Analytic bounds	46
3.5 Summary	49

4. Array Processing with Space-Time Block Codes	50
4.1 Performance Analysis of BLAST	52
4.1.1 Effect of error propagation in BLAST	54
4.1.2 Performance of BLAST in correlated fading	57
4.2 Multilayered Space-Time Coding	64
4.3 Combining STBC and BLAST	69
4.4 Transmit Beamforming and Space-Time Coding	73
4.5 Summary	76
5. Conclusions	77
5.1 Summary of Results	77
5.2 Future Work	78
Bibliography	79
Vita	85

List of Figures

2.2.1	Schematic of a system using STBC	11
2.2.2	Performance of STBC in uncorrelated Rayleigh fading (1bps/Hz)	15
3.1.1	Illustration of wireless propagation environment	21
3.2.1	Geometrically based circular channel model	24
3.2.2	Covariance Matrix of Circular channel model for various transmit antenna separations	29
3.2.3	Variation of correlation with Tx antenna spacing in a circular channel model	30
3.2.4	Variation of correlation with angle spread	31
3.2.5	Correlation of various antenna elements with the first antenna in an 8 element linear array for the circular model	32
3.3.1	Geometrically based elliptical channel model	33
3.3.2	Covariance Matrix of Elliptical channel model for various Tx antenna separations	37
3.3.3	Variation of correlation with Tx antenna spacing in an elliptical channel model	38
3.3.4	Ellipses in which uniformly distributed scatterers cause flat fading	39
3.3.5	Distribution of angle spread in an elliptical channel for various transmit receive distances	39
3.3.6	Variation of correlation with Transmit – Receive distance in an elliptical channel model	40
3.4.1	Performance of G2 – STBC in Circular Channel (Effect of Transmit element spacing)	42
3.4.2	(a) Performance of G4 STBC in Circular model (1Rx antenna)	43
3.4.2	(b) Performance of G4 STBC in Circular model (2 Rx antennas)	43
3.4.3	Effect of Angle Spread on the Performance of G2 STBC in circular model (2Rx Antennas)	44

3.4.4	Performance of G2 STBC in elliptical model (Effect of geometry of ellipse)	45
3.4.5	Performance of G4 STBC in elliptical model (Effect of geometry of ellipse)	46
3.4.6	(a) Comparison of Analytic and Simulated results for G2 STBC in circular channel	47
3.4.6	(b) Comparison of Analytic and Simulated results for G4 STBC in circular channel	47
3.4.7	(a) Comparison of Analytic and Simulated results for G2 STBC in elliptical channel	48
3.4.7	(b) Comparison of Analytic and Simulated results for G4 STBC in elliptical channel	48
4.1.1	V-BLAST Scheme	52
4.1.2	(a) BER of Individual BLAST layers without error propagation (8Tx – 8Rx)	55
4.1.2	(b) BER of Individual BLAST T layers with error propagation (8Tx – 8Rx)	56
4.1.3	Effect of error propagation on BLAST (8Tx – 8Rx)	57
4.1.4	A 2X2 MIMO channel	57
4.1.5	(a) Performance of BLAST with MMSE suppression in the presence of only transmit correlation	59
4.1.5	(b-e) Covariance matrices of 4X4 MIMO channel model with only transmit correlation. For (b) $ \mathbf{r}_{Tx} = 0.0$; for (c) $ \mathbf{r}_{Tx} = 0.25$; for (d) $ \mathbf{r}_{Tx} = 0.70$; for (e) $ \mathbf{r}_{Tx} = 0.80$. Correlation between all other paths is less than 0.1	59
4.1.6	(a) Performance of BLAST with MMSE suppression in the presence of only receive correlation	60
4.1.6	(b-e) Covariance matrices of 4X4 MIMO channel model with only receive correlation. For (b) $ \mathbf{r}_{Rx} = 0.0$; for (c) $ \mathbf{r}_{Rx} = 0.25$; for (d) $ \mathbf{r}_{Rx} = 0.70$; for (e) $ \mathbf{r}_{Rx} = 0.80$. Correlation between all other paths	

is less than 0.1	60
4.1.7 Comparison between the effect of transmit and receive correlation in MMSE-BLAST	61
4.1.8 (a & b) Covariance matrices of 4X4 GBSB-MIMO channel models. For Channel A shown in 4.1.8(a) $r_{\max} = 0.3$. For Channel B shown in 4.1.8(b) $r_{\max} = 0.4$	62
4.1.8 (c) Performance of MMSE-BLAST in general correlated channels	63
4.1.9 Distribution of the condition number (in dB scale) for the channel matrices representing Channel A and Channel B	64
4.2.1 Comparison of BLAST and Multilayered STC with Space-Time Block codes over each group	68
4.3.1 Performance of BLAST with STBC layers (4Tx – 4Rx, QPSK)	71
4.3.2 Performance of BLAST with STBC layers (4Tx – 4Rx, QPSK) in correlated fading	72

Chapter 1

Overview and Contributions

1.1 Overview

Wireless systems are developing rapidly to provide voice, data and multimedia messaging services. These services require reliable wireless channels with large capacities. Systems which communicate over a Single Input Single Output (SISO) wireless channel¹ have limited capacity. Also, in some situations, communication over a SISO channel is not reliable due to multipath fading. Information theoretic investigations in the past few years [Fos96], [Fos98] have shown that very high capacities can be obtained by employing multiple antenna elements at both the transmitter and the receiver of a wireless system. Results of these investigations led to the development of a novel transmit-receive architecture called Bell Labs Layered Space-Time Architecture (BLAST) [Fos96] which provides transmission rates that are unattainable by using traditional techniques. Another approach that uses multiple transmit and if possible multiple receive antennas to provide reliable and high data communication is Space-Time Coding (STC) [Tar98], [Tar99a]. BLAST and STC make use of both the space (different antennas) and the time domain while encoding and decoding information symbols. Hence, the phrase space-time coded modulation can be generically applied to both techniques.

¹ SISO channel has a single transmit antenna and a single receive antenna.

The introduction of BLAST and STC has encouraged researchers in the wireless field to identify and study the various issues involved in providing high data rate wireless communication using multielement antennas. Key areas of investigation include: developing MIMO² vector channel models which can characterize signals at different antennas at both ends of the wireless link, designing efficient upper layer (data link layer, network layer) algorithms which can utilize the benefits of multielement antenna transmission, combining other communication techniques like OFDM with different multi-antenna transmission schemes and studying the effect of system level impairments like multiple access interference on these schemes. The objective of this thesis is to develop MIMO channels which model correlated fading and analyze the performance of space-time coded modulation schemes in these channel models.

1.2 Outline of Contents

The thesis is organized as follows. Chapter 2 begins with a brief description about the current research on various channel models which are being used to characterize the performance of MIMO schemes. Then, methods of transmitting from multiple antennas³ are introduced. Later, a detailed description of the basic features of Space-Time Block Coding (STBC), a popular transmit diversity scheme is given. Finally, the last part of the chapter provides a brief overview of transmit diversity techniques which will be incorporated in 3G wireless systems.

Chapter 3 gives details about modeling the fading correlation between various antenna elements in a MIMO system by using Geometrically Based Single Bounce (GBSB) vector channel models. The procedure to model fading correlation initially formulated in [Shiu00] is used here in conjunction with prior work done on GBSB models [Ert98a], [Lib96]. Channel models described in this chapter attempt to model two different ‘realistic’ scenarios: one without scatterers around the transmitter and the other with scatterers around the transmitter. Performance of STBC in these ‘GBSB-MIMO’ models

² MIMO stands for Multiple Input Multiple Output.

³ Methods of transmitting from multiple transmit antennas are usually called transmit diversity techniques.

is then studied for various conditions. Finally, the BER curves generated using simulations are validated by using analytic expressions which were derived in [Goz02b].

Chapter 4 starts with a brief introduction to BLAST and analyzes its performance in correlated MIMO channels. Fundamentals of multilayered space-time coded modulation [Tar99b] are presented next. This scheme combines the concepts of BLAST and STC. Principles of multilayered space-time coded modulation are then applied with Space-Time Block codes to arrive at schemes which can provide reasonably high spectral efficiencies at a reasonably low SNR. Performance of these schemes is also analyzed in correlated MIMO channels. Finally, the chapter presents a discussion on various issues involved in combining beamforming and space-time coding at the transmitter.

Chapter 5 summarizes the thesis and presents a brief discussion on possible research directions which can extend the investigations presented in this work.

1.3 Contributions

The contributions of this thesis are

- Extending the work presented in [Shiu00] on modeling fading correlation in multielement antenna systems to urban microcell scenarios where scatterers are present around the base station. This is done by considering an elliptical distribution of scatterers [Lib96] with the transmitter and the receiver located at the foci of the ellipse.
- Analyzing the performance of space-time block codes in GBSB-MIMO models for suburban and urban microcell scenarios using Monte Carlo simulations and validating these results with analytical expressions derived in [Goz02b]. This work is submitted for publication as a section in [Goz02c].
- Studying the sensitivity of BLAST scheme to spatial correlation and comparing this with the sensitivity of space-time block codes.

- Employing the concepts of ‘multilayered space-time coding’ which was initially presented in [Tar99b] to design schemes that use transmit diversity in the form of space-time block codes to improve the power efficiency of BLAST and, study the robustness of these schemes to spatial correlation.

Chapter 2

Introduction to Space-Time Block Codes

Schemes which use multiple transmit and receive antennas for communicating over a wireless channel are usually called Multiple Input Multiple Output (MIMO) schemes. This chapter gives an introduction to Space-Time Block Coding (STBC); a technique used to transmit symbols from multiple antennas. The chapter is organized as follows.

Section 2.1 gives a brief description about the current research on various channel models which are being used to characterize the performance of MIMO schemes. Section 2.2 introduces transmit diversity and provides a detailed description of the basic features of Space-Time Block Codes. Section 2.3 gives a brief overview of various transmit diversity techniques that are proposed for future wireless systems. Section 2.4 concludes the chapter with a brief summary of the material presented.

2.1 Multiple Input Multiple Output (MIMO) channels

To effectively evaluate the performance of a MIMO transmission scheme, models which account for all the major effects of wireless channel on various signals are required. The most commonly used channel model for MIMO systems is independent quasi-static flat Rayleigh fading at all antenna elements. This was employed in [Fos96], [Ala98], [Tar98], [Tar99a], and [Tar99b] where novel signal processing schemes for MIMO systems were introduced. The simplicity of this channel model made the performance analysis of these schemes less complicated, allowing the authors to place more emphasis on introducing

the transmit and receive signal processing algorithms. Fundamental Information theoretic results on capacity of MIMO channels [Fos98] and transmit diversity techniques [Ara99] also employ a similar fading channel model.

The basic assumptions behind the independent quasi-static flat Rayleigh fading channel are

- A large number of scatterers are present in the wireless channel so that the signal at any receive antenna of the MIMO system is the sum of several multipath components. In this case the distribution of the received signal at each antenna will be complex Gaussian. The amplitude of such complex Gaussian distributed signals is Rayleigh distributed.
- The channel delay spread, which is a measure of the difference in the TOA of various multipath components at the receiver antenna, is less than the symbol rate. This assumption guarantees flat fading.
- The channel characteristics remain constant at least for the period of transmission of an entire frame. This assumption accounts for quasi-static fading.
- The antenna elements at the transmitter and the receiver of the MIMO system are placed far enough (spatially) such that the effect of the channel at a particular antenna element is different from the effect at all other antenna elements. This supports the assumption of independent or spatially uncorrelated fading.

Using all these assumptions, the independent quasi-static flat Rayleigh fading MIMO channel for a system with n_T transmit and n_R receive antennas can be represented as

$$H = \begin{bmatrix} h_{1,1} & h_{1,2} & \cdots & h_{1,n_T} \\ h_{2,1} & h_{2,2} & \cdots & h_{2,n_T} \\ \vdots & \vdots & \ddots & \vdots \\ h_{n_R,1} & h_{n_R,2} & \cdots & h_{n_R,n_T} \end{bmatrix} \quad (2.1)$$

where $h_{i,j}$ is the path gain. This is the effect of the channel on signals transmitted from j^{th} transmit antenna and received at the i^{th} receive antenna. As H is a Rayleigh flat

fading MIMO channel the path gains are usually modeled as zero mean independent complex Gaussian random variables with variance 0.5 per real dimension.

As research on MIMO schemes progressed, focus on more elaborate MIMO channel modeling increased. The assumption that fading at various antenna elements is spatially uncorrelated was found too simplistic in many realistic scenarios. Thus, channel models were designed to account for spatial correlation.

Analysis of spatial correlation across Base Station (BS) antenna elements in systems with single transmit antenna and multiple receive antennas¹ has been widely considered for diversity arrays. Initial results in this area were obtained by Lee in [Lee73] by using a geometrically based scattering model. The effect of fading correlation at base station antennas on diversity combining was studied in [Salz94] by using a channel model similar to the one used by Lee. More recently analytic models for spatial correlation as a function of angle spread of the signals arriving at an array were reported in [Dur99] and [Bue00].

Channel models for MIMO systems were presented in [Shiu00], [Gesb00a], [Chiz00a], [Alex01], [Moli02a] and [Moli02b]. In [Chiz00a] and [Alex01] statistical MIMO channel models are used to study the effect of correlation on the capacity of BLAST and the BER of space-time block codes respectively. Here the authors assume that the base station is located far away from scatterers while the mobile is in a rich scattering environment.

In [Shiu00], a comprehensive treatment on the capacity of MIMO systems in correlated fading channels is presented. The correlated MIMO channels are obtained by extending Lee's geometrically based model to multielement antenna systems. The authors show that the capacity of a MIMO channel is dependant on the eigen-values of HH^\dagger where H is the channel matrix. The capacity is given as

¹ These systems are usually called as Single Input Multiple Output – SIMO systems.

$$C = \sum_{k=1}^n \log_2 \left(1 + \frac{\rho}{n_T} \epsilon_k^2 \right), \quad (2.2)$$

where n is the number of eigen-values of HH^\dagger , ρ is the average SNR and ϵ_k^2 is the k^{th} eigen-value of HH^\dagger . It is clear from (2.2) that the capacity of a MIMO channel can be treated as a sum of capacities of n SISO sub-channels with the power gain for each channel being ϵ_k^2 . If all the elements of H are uncorrelated then all values of ϵ_k^2 for $k = 1, 2, \dots, n$ will have a significant value. However when elements are correlated some eigen-values may be nearly zero, thus reducing capacity.

Discussion in [Shiu00] showed that capacity decreases when the signals at various antennas are correlated. However, having uncorrelated fading at the transmit and receive elements does not guarantee high capacity. In certain situations only a single eigen-mode for propagation can exist even when elements of the channel matrix are uncorrelated. These special scenarios are called ‘keyholes’ [Chiz00b], [Chiz02] or ‘pinholes’ [Gesb00a] and [Gesb00b]. The probability of occurrence of these keyholes is usually low but cannot be ruled out in realistic scenarios like propagation in corridors for indoor environments and diffraction caused at roof edges for outdoor environments.

Generic models which account for all important propagation effects in the channel including keyholes are presented in [Moli02a] and [Moli02b]. These models employ ‘double scattering’ propagation processes. The references also attempt to parameterize the various possible effects which can completely define a MIMO model.

Measurement campaigns can be used to practically characterize MIMO environment and verify the applicability of various channel models. MIMO channel measurements for indoor environments are reported in [Bat01] and [Stoy01]. Measurements for outdoor MIMO channels are reported in [Bat02].

2.2 Fundamentals of Space-Time Block Coding

This section introduces the basics of Space-Time Block Coding (STBC). The section begins with an overview of various transmission schemes for multielement antenna systems. Following this, the structure of various STBC encoders and decoders is explained and their performance is characterized.

2.2.1 Introduction to Transmit Diversity schemes

In a system with multiple transmit antennas, information can be transmitted by employing various transmission techniques. One way is to transmit a weighted version of the same information symbol from all the antennas. The weights can be adjusted to compensate for the distortion caused by the downlink channel on transmit signals. This method is called *transmit beamforming* and requires the receiver to estimate the downlink channel and feed back this information to the transmitter from time to time [Ger94]. Another alternative is to use *antenna selection* where only a single antenna is used for transmission at any particular instant [Wint83]. This scheme would also need feedback. However, antenna selection methods based on very little feedback information where the receiver only tells which subset of available antennas should be used for transmission were proposed recently [Hea01a], [Blum02]. Nevertheless, providing a separate feedback link not only makes the signaling protocol more elaborate but also increases the complexity at the receiver.

Transmission schemes which do not require downlink channel estimation are usually called as open loop transmit diversity techniques. In these schemes, all antennas transmit simultaneously. As downlink channel information is not available, usually the total transmit power is distributed equally among all the antennas. Open loop schemes have less complex signaling formats and are easier to implement in practical systems.

Space-Time Coding (STC) is an open loop transmission scheme that was introduced in [Tar98]. In STC, joint design of channel coding and modulation is done to create efficient transmission techniques which improve system performance by providing both the diversity advantage of multiple transmit antennas and coding gain. In [Tar98], space-time codes based on trellis-coded modulation (TCM) are presented. These codes are called Space-Time Trellis Codes (STTC) and their performance was shown to be very good in slow Rayleigh fading environments. The receiver for these STTC schemes uses Maximum Likelihood Sequence Estimation (MLSE) and the decoding complexity for these schemes (measured in terms of number of trellis states) increases exponentially with transmission rate for a fixed number of transmit antennas.

[Ala98] introduced a simple open loop scheme which provides a transmit diversity gain similar to that obtained by using Maximal Ratio Combining (MRC) in receive diversity systems. This scheme was proposed for two transmit antennas. Symbols transmitted from these antennas are encoded in space and time in a simple manner to ensure that transmissions from both the antennas are orthogonal to each other. This would allow the receiver to decode the transmitted information with very little additional computational complexity even if it has a single antenna element. Using the theory of orthogonal designs, the simple scheme proposed in [Ala98] was generalized to systems with more than two transmit antennas [Tar99c]. These generalized schemes were called Space-Time Block Codes (STBC) [Tar99a].

Since the transmissions from various antennas elements are orthogonal, space-time block codes provide additional transmit diversity at the receiver. However, they don't provide a significant coding gain. Concatenating space-time block codes with an outer of layer trellis codes combines the coding gain of trellis codes with the diversity gain of STBC. It was shown that the performance of such combined schemes is similar to, or even better than STTC [Sand01].

2.2.2 Encoding and decoding of Space-Time Block codes

The structure of a system employing space-time block codes is shown in Figure 2.2.1. Here, at a given time instant t , the transmitter maps a block of kb bits into a block of k information symbols $s_t^1 s_t^2 \dots s_t^k$. Each symbol belongs to the 2^b element signal constellation used at transmitter. Symbols are then encoded in space (across different antennas) and time (across various symbol periods). The manner in which symbols are

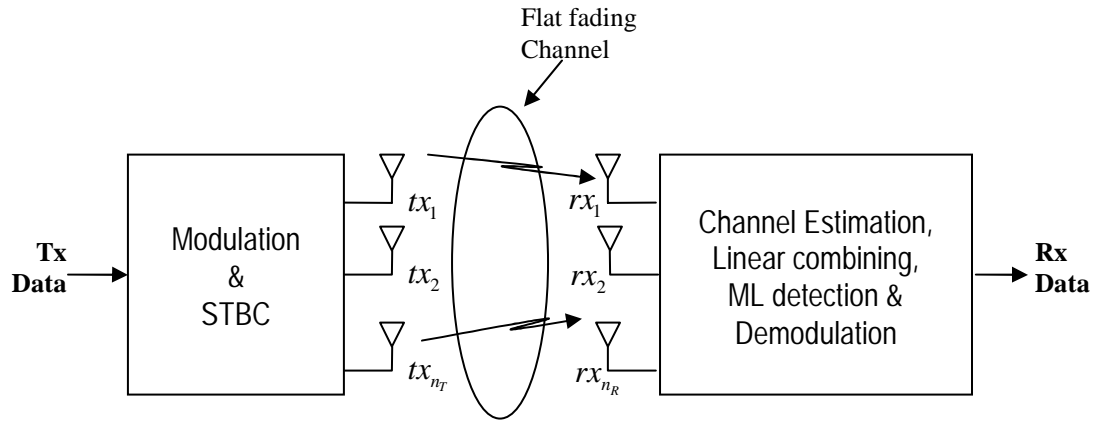


Figure 2.2.1 Schematic of a system using STBC

encoded is determined by a specific code matrix, usually denoted by G_{n_T} or H_{n_T} . The matrix has n_T columns and p rows. Each block of k information symbols is encoded using this $p \times n_T$ matrix. After encoding, all space-time block coded symbols corresponding to a particular row of the encoder matrix are transmitted in one symbol period. Since p symbol intervals are utilized in transmitting k information symbols, the code rate R for a particular $p \times n_T$ encoder matrix is given by $R = k/p$. It should be noted that at any given time instant t , n_T space-time block coded symbols $c_t^1 c_t^2 \dots c_t^{n_T}$ are transmitted.

Assuming a Quasistatic flat Rayleigh fading channel (see section 2.1), the received signal at the j^{th} receive antenna can be given as²

$$r_t^j = \sum_{i=1}^{n_r} h_{i,j} c_t^i + \eta_t^j, \quad (2.3)$$

where η_t^j accounts for AWGN noise at j^{th} receive antenna. Noise terms are modeled as independent samples of a zero mean complex Gaussian random variable with variance $\frac{n_r}{2SNR}$ per complex dimension. The receiver performs ML decoding of these space-time coded transmissions by using some simple linear processing operations.

For example in a scenario with two transmit antennas, the STBC encoder matrix is

$$G_2 = \begin{bmatrix} x_1 & x_2 \\ -x_2^* & x_1^* \end{bmatrix}. \quad (2.4)$$

This is a full rate ($k=1$) code since two information symbols are transmitted in two symbol durations. If the information symbols are s_1 and s_2 , then in the first time slot (which is one symbol duration) the transmitter sends s_1 from antenna 1 and s_2 from antenna 2 simultaneously. In the second time slot $-s_2^*$ and s_1^* are transmitted simultaneously from antennas 1 and 2 respectively.

The receiver uses maximum likelihood detection to decode the symbols. For G_2 STBC, it minimizes the decision metric

$$\sum_{j=1}^{n_R} \left| r_1^j - h_{1,j} s_1 - h_{2,j} s_2 \right|^2 + \left| r_2^j - h_{1,j} s_2^* - h_{2,j} s_1^* \right|^2 \quad (2.5)$$

over all possible s_1 and s_2 , and the values of s_1 and s_2 which minimize the decision metric are receiver estimates of the transmitted symbols. Equation (2.5) can be split into

² Here the received signal is in the complex base band representation.

two different expressions for minimization, for detecting s_1 and s_2 respectively. The decision metric

$$\left| \left[\sum_{j=1}^{n_R} \left(r_1^j h_{1,j}^* + (r_{2,j})^* h_{2,j} \right) \right] - s_1 \right|^2 + \left(-1 + \sum_{j=1}^{n_R} \sum_{i=1}^2 |h_{i,j}|^2 \right) |s_1|^2 \quad (2.6)$$

should be minimized for decoding s_1 and

$$\left| \left[\sum_{j=1}^{n_R} \left(r_1^j h_{2,j}^* + (r_{2,j})^* h_{1,j} \right) \right] - s_2 \right|^2 + \left(-1 + \sum_{j=1}^{n_R} \sum_{i=1}^2 |h_{i,j}|^2 \right) |s_2|^2 \quad (2.7)$$

should be minimized for decoding s_2 . For the case of three transmit antennas, the encoder matrix denoted by G_3 is shown in (2.8). The code rate of this matrix is $k = 0.5$ as four information symbols are transmitted in eight symbol periods. An alternate STBC design for three transmit antennas which provides a higher code rate $k = 0.75$ is given in [Tar99b].

$$G_3 = \begin{pmatrix} x_1 & x_2 & x_3 \\ -x_2 & x_1 & x_4 \\ -x_3 & x_4 & x_1 \\ -x_4 & -x_3 & x_2 \\ x_1^* & x_2^* & x_3^* \\ -x_2^* & x_1^* & x_4^* \\ -x_3^* & x_4^* & x_1^* \\ -x_4^* & -x_3^* & x_2^* \end{pmatrix} \quad (2.8)$$

The encoding matrix for transmitting from four antennas is given in (2.9). The code rate for this scheme too is $k = 0.5$. Similar to the three transmit antenna case, a scheme with $k = 0.75$ is also available for four transmit antennas and is given in [Tar99b].

$$G_4 = \begin{pmatrix} x_1 & x_2 & x_3 & x_4 \\ -x_2 & x_1 & -x_4 & x_3 \\ -x_3 & x_4 & x_1 & -x_2 \\ -x_4 & -x_3 & x_2 & x_1 \\ x_1^* & x_2^* & x_3^* & x_4^* \\ -x_2^* & x_1^* & -x_4^* & x_3^* \\ -x_3^* & x_4^* & x_1^* & -x_2^* \\ -x_4^* & -x_3^* & x_2^* & x_1^* \end{pmatrix} \quad (2.9)$$

For decoding G_3 and G_4 , decision metrics whose structure is similar to that given in (2.5) need to be computed. Details for decoding G_3 and G_4 are given in Appendix A.

2.2.3 Performance of Space-Time Block coding

As mentioned earlier, space-time block coding ensures that transmissions from various antennas are orthogonal. This allows even a single element receiver to exploit a transmit diversity gain which is similar to the gain obtained by using Maximal Ratio Combining (MRC) in multiple receive antenna systems. The advantage of space-time codes lies in the fact that diversity advantage is obtained by shifting the complexity of adding additional antennas to the transmitter while allowing the complexity of receiver to be reasonably low.

The spectral efficiency of STBC schemes depends on the type of modulation and the coding scheme which is employed. For example G2 – QPSK (G2 space-time block coding scheme with QPSK modulated symbols) transmits at 2bps/Hz as four information bits (two QPSK symbols) are sent in every two symbol intervals. On the other hand G4 – QPSK transmits at 1bps/Hz as it takes eight symbol intervals to send eight information bits (four QPSK symbols).

Performance of space-time block codes is illustrated in Figure 2.2.2. Bit error rate (BER) curves for transmission using two and four transmit antennas are shown in this figure. The x-axis of the plots represents the SNR per bit at the receiver. Unless noted otherwise,

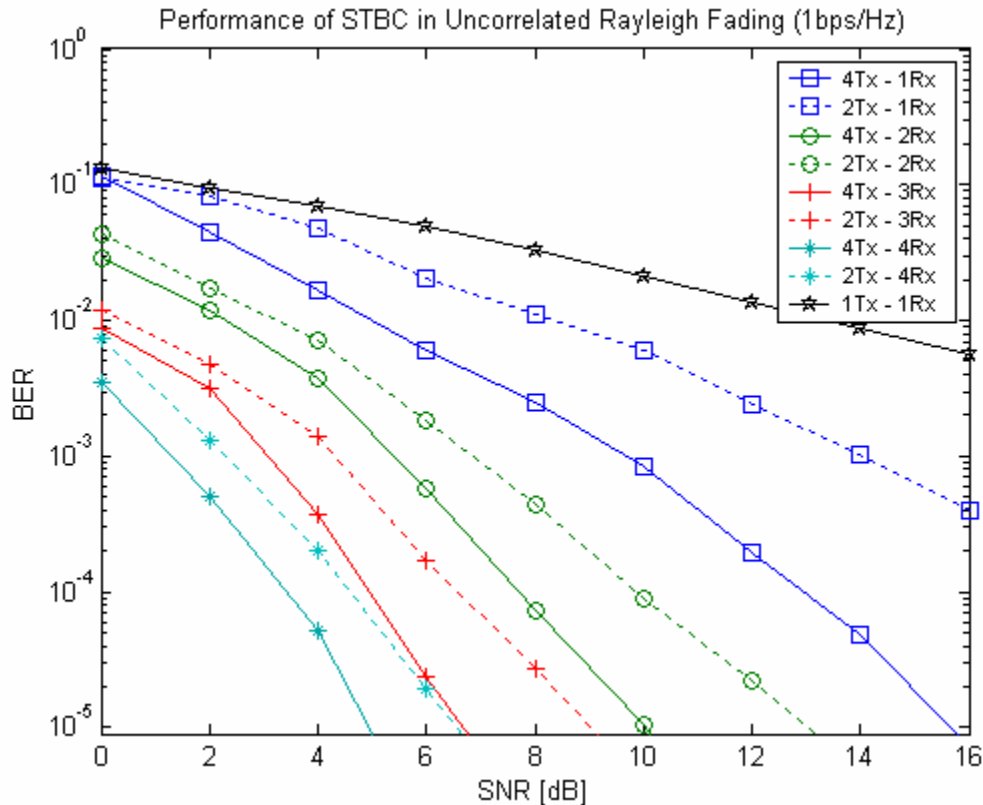


Figure 2.2.2 Performance of STBC in uncorrelated Rayleigh fading (1bps/Hz)

the x-axis of all the BER plots in the remainder of this thesis follows the same representation. G2 - BPSK is used for the two antenna case and G4 - QPSK for four antenna case so that the transmission is at 1bps/Hz in both scenarios. The BER curve for the one transmit and one receive antenna (1Tx-1Rx) case is also plotted for reference. The following observations can be made from the performance plots.

Firstly, the plots indicate that that using space-time block codes improves the diversity order at the receiver. This can be inferred since the slope of the BER curve for 2Tx-1Rx case is steeper than the 1Tx-1Rx case as the former has a second order diversity advantage. Similarly the slope for 4Tx-1Rx case is steeper than 2Tx-1Rx case as its diversity order is greater.

The plots also illustrate that for the same diversity order, the scheme with more receive antennas gives better performance. This is because, when the number of transmit

antennas is increased, the transmitted power from each individual antenna is less, since the total available transmit power is constant and is divided equally among all the antennas. This effect is illustrated by the BER curves for the 4Tx-1Rx and 2Tx-2Tx cases. Both scenarios have the same diversity order (BER plots have same slope) but the BER performance for 2Tx-2Rx case is 3dB better.

Finally, plots also show that the additional diversity advantage obtained by increasing the number of antenna elements diminishes as more and more elements are added. For instance at a BER of 10^{-5} , the performance of 4Tx-2Rx is nearly 6dB better than 4Tx-1Rx. Adding an other receive antenna improves the performance by about 3.5dB and adding one more receive antenna gives only an extra 1.75dB gain in performance.

Correlation between signals of different antenna elements at both the transmitter and the receiver affects the performance of space time block codes to a large extent. The effect of correlation on the performance of space-time block codes was initially investigated in [Rens00]. In [Goz02] the analysis was extended to arrive at a closed form expression to calculate the upper bounds on symbol error probability of various STBC schemes with M-ary PSK modulation. The analytic expression is

$$P_e \leq \sum_{m=1}^{n_T n_R} a_m \left[1 - \frac{1}{\sqrt{1 + \frac{2}{\lambda_m \gamma_{eq}}}} \right], \quad (2.10)$$

where, λ_m is the m^{th} eigen-value of covariance matrix of the channel H . If the columns of H are stacked one below each other to obtain a vector $\text{Vec}H$ then covariance matrix is computed using $\text{Cov}H = \text{Vec}H \text{Vec}H^\dagger$. a_m and γ_{eq} are given by

$$a_m = \frac{\lambda_m^{n_T n_R - 1}}{\prod_{l=1}^{n_T n_R} (\lambda_m - \lambda_l)}, \lambda_l \neq \lambda_m,$$

$$\gamma_{eq} = \frac{2(E_s/N_o) \sin^2\left(\frac{\pi}{M}\right)}{kn_T}.$$

$\frac{E_s}{N_o}$ is the SNR per symbol at the receiver, M is the number of points in the constellation of the PSK scheme and k is code rate of the space-time block code.

A more detailed performance analysis of STBC in realistic channels with correlated fading is presented in Chapter 3.

2.3 Transmit Diversity Techniques for 3G wireless systems

Employing antenna diversity is one of the many ways being used to increase the capacity of next generation wireless systems. Current generation cellular standards like, IS-136 and IS-95 support antenna diversity on the uplink by using multiple antennas at base stations to receive signals. To improve signal quality on the downlink, transmit diversity is an attractive option as it improves signal quality without adding additional antennas at the mobile. Space-time block codes have the advantage that they provide diversity improvement without significantly increasing the complexity at the receiver. Due to this characteristic, both the two major 3G wireless standards, WCDMA and IS-2000, have incorporated modified versions space-time block coding as a means of providing transmit diversity. This section gives a brief description of these modified schemes.

Transmit Diversity in WCDMA systems

Two open-loop transmit diversity schemes are supported by WCDMA; Time Switched Transmit Diversity (TSTD) and Space-Time Transmit diversity (STTD) [3GP01]. TSTD is a simple scheme where symbol transmissions are switched from one antenna to another antenna in a periodic fashion. In the case of two transmit antennas all even symbols are transmitted from antenna 1 and all the odd symbols are transmitted from antenna 2. TSTD is proposed for downlink transmissions on the synchronization channel of WCDMA.

The STTD scheme is an extension of the simple transmit diversity method proposed in [Ala98] to CDMA type wideband systems. QPSK modulated symbols are space-time block coded using G2 before Walsh modulation and long code spreading.

WCDMA also supports closed loop transmit diversity [3GP02]. The feed back information from the receiver can be as little as which transmit antenna to choose, such as in Selective Transmit Diversity (STD) or it can be more elaborate such as in Transmit Adaptive Arrays (TxAA).

Transmit Diversity in IS-2000 systems

IS-2000 supports two different open loop transmit diversity schemes. The first scheme is Orthogonal Transmit Diversity (OTD) and the other scheme is Space Time Spreading (STS). STS employs the concepts of [Ala98] to maintain orthogonality between signals from different transmit antennas while OTD relies on using orthogonal Walsh spreading codes at different antennas. In a two transmit antenna scenario, STD provides a two fold path diversity gain while OTD provides only single path diversity. The encoding and decoding of STS is slightly more complex than that of OTD.

2.4 Summary

This chapter has introduced certain basic aspects of MIMO systems, such as the channel modeling and transmission from multiple antennas. The chapter also provided details of encoding and decoding for space-time block coding; a popular transmit diversity mechanism. These codes enable mobile receivers to exploit transmit diversity with very little increase in complexity. Standards for 3rd Generation wireless systems, WCDMA and IS-2000 have incorporated modified versions of space-time coding as a means to provide transmit diversity. The final section of the chapter briefly introduced these modified schemes.

Chapter 3

Performance Analysis of Space-Time Block Codes in GBSB-MIMO Channel Models

Performance of space time block codes depends to a large extent on correlation between signals of different antenna elements at both the transmitter and the receiver. Performance results presented during the early stages of research on Space Time Block Codes (STBC) were based on the assumption that fading between different antenna elements is independent [Tar99a]. This assumption provides the best possible diversity scenario and is reasonably valid in rich a scattering environment which is usually seen in indoor scenarios. However in outdoor channels, significant correlation can exist between antenna elements (Especially between different elements of transmit base station arrays). This would negatively affect the performance of STBC as fewer dissimilar replicas of the same signal are generated.

The effect of correlation between various antenna elements on the capacity of MIMO systems has been investigated in [Shiu00]. Here the authors use a ‘one ring abstract channel model’ to characterize fading correlation. More recently [Alex01] employed a ‘stochastic geometry-based’ model to study effects of correlation on the performance of Space Time Block codes. The channel models used in both these works assume that the transmitter is located far from any scatterers while the receiver is in a rich scattering environment, which is generally the case in rural and sub urban scenarios with tall base station antennas.

This chapter gives details about modeling the fading correlation between various antenna elements in a MIMO system by using Geometrically Based Single Bounce (GBSB) vector channel models. The procedure to model fading correlation initially formulated in [Shiu00] is used here in conjunction with prior work done on GBSB models [Ert98a], [Lib96]. The channel models described in this chapter attempt to model two different ‘realistic’ scenarios; one without scatterers around the transmitter and the other with scatterers around the transmitter (resembling situations for base stations at lower heights in urban microcell environments). Performance of various STBC schemes in these ‘GBSB-MIMO’ models is then characterized by using bit error rate (BER) curves. These BER curves are obtained by running Monte Carlo simulations over a large number of GBSB-MIMO channel realizations. Finally, the BER curves generated using simulations are validated by using analytic expressions given in [Goz02b]. These expressions calculate upper bounds for STBC error probability using the channel covariance matrix.

Section 3.1 of this chapter provides a basic overview of GBSB vector channel modeling. Section 3.2 explains the geometrically based Circular Channel model which is normally used to characterize scenarios where the transmitter is placed far away (or above) from any possible scatterers. The receiver in this model assumed to be surrounded by scatterers uniformly distributed within a circle. Section 3.3 deals with the Elliptical Channel model where both the transmitter and receiver are located amidst scatterers which are uniformly distributed in an ellipse. Simulation results which illustrate the performance of Space Time Block Codes in these channel models are presented in Section 3.4.

3.1 Introduction to GBSB channel models

When a signal is transmitted through a wireless medium it interacts with the environment in several ways (see Figure.3.1.1). Large objects in the path of signal transmission may obstruct the signal, cause diffraction or reflect it in a certain direction. Smaller objects can scatter the signal energy in various random directions [Rap96], [Ert98a]. Due to all these effects the receiver may see various copies of the signal arriving through different paths with each path distorted differently.

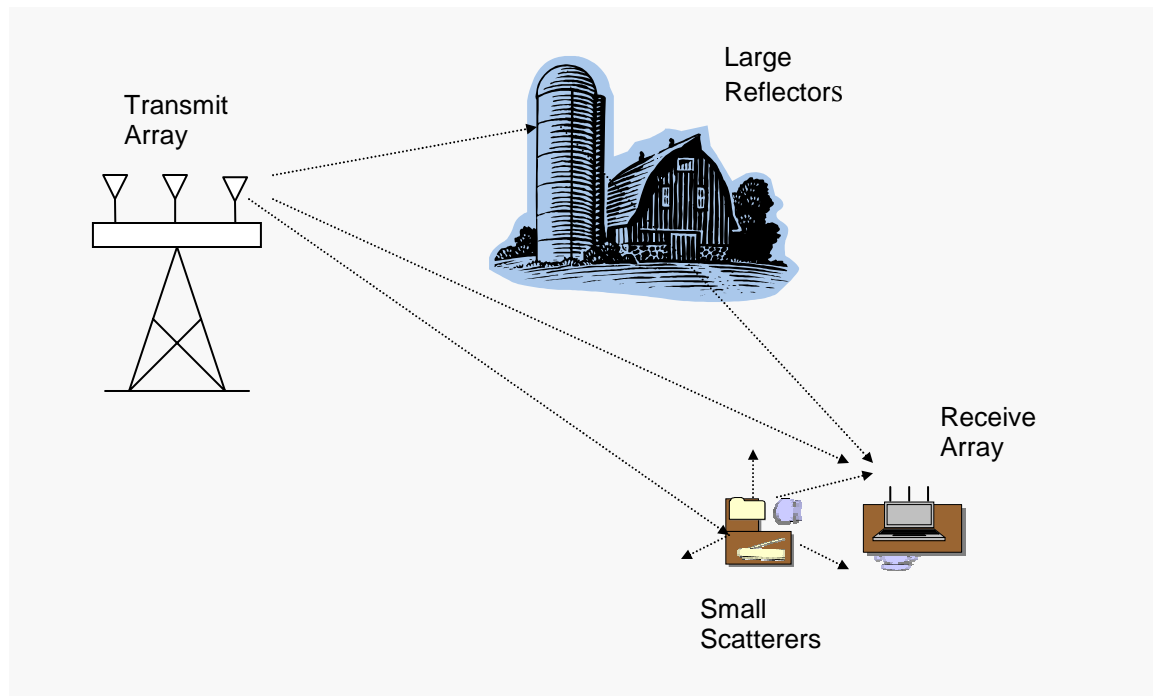


Figure 3.1.1 Illustration of wireless propagation environment

Channel models for wireless environments should be able to depict the effect of all these interactions and predict the received signal characteristics so that they resemble the actual characteristics as closely as possible. However, exact or even near exact modeling of the channels can be very complex and is not possible unless detailed prior information about the channel environment and the transmitted signal structure is available [Tra92]. In most cases, channel models are used to predict the general nature of the received signal by providing information about certain parameters like the distribution of its amplitude and phase, the Doppler shift caused due to relative motion between objects in the channel and the transmitter or receiver, the angle of arrival/departure of signals at the transmitter and the receiver etc. These parameters are then used in simulations to study the performance of various communication algorithms. An overview of various channel models is given in [Ert98b].

In order to model the fading correlation between signals of various antenna elements in a MIMO system, we need to employ a channel structure which generates the characteristics

of received signals according to the nature of wireless environment in which the system is operating. A good way to do this is to employ geometrically based channel models which use information about the physical locations of the transmitter, receiver and various objects present in the surrounding environment. These models combine this geometric information with ray tracing techniques to model the characteristics of signals at various antenna elements of transmitter and receiver. Exact locations of objects in the channel cannot be usually determined for all possible scenarios. Hence, the geometrically based models assume that objects are located according to a particular geometrical distribution, which closely resembles the realistic situation which is being modeled.

In Geometrically Based Single Bounce (GBSB) models, the signals at the receiver antennas are modeled as a summation of various rays starting at the transmitter and arriving at the receiver. Each ray is assumed to be reflected only once by a scatterer in its path to the receiver. In the case of MIMO systems, signals at each antenna element of the receiver are the sum of scattered rays from all the transmit antenna elements. Rays which are reflected more than once are not considered in these models. Normally, when a signal ‘bounces’ on an object, it dissipates some of its energy (this can be due to absorption by the material or scattering), so signals arriving at the receiver after multiple reflections have much smaller energy and thus have less effect on system performance.

The basic advantage of using GBSB models in our simulations is that they provide a framework through which correlations between various antenna elements can be manipulated by changing physical parameters of the system. For example, it’s known that increasing spacing between elements of the transmit antenna array would generally reduce the correlation. By using an appropriate GBSB model we can actually predict how far the elements should be separated to keep the correlation between adjacent antenna elements below a particular value.

All physical scenarios cannot be modeled by changing the parameters of a single geometrical distribution. Different geometries of scatterer distributions and transmitter/receiver locations are needed to model different scenarios. Two such

geometries are described in the next two sections of this chapter. While using GBSB models the following assumptions are made [Lib96], [Ert98a], [Shiu00].

1. All scatterers are assumed to be in the same plane as the transmitter and receiver. Hence, no vertical component exists for the propagating rays. This is not true for most realistic scenarios. However, using 2D models makes the analysis more tractable and the models can easily be extended to three dimensions.
2. When a ray is impinged on a scatterer its energy is reradiated equally in all directions.
3. Each scatterer is associated with a random phase ϕ . This phase is modeled as a uniform random variable distributed in $[-\pi, \pi]$. This is done to account for the dielectric properties of the scatterers [Lee73].
4. Rays which reach the receiver after getting reflected only once by a particular scatterer are considered for analysis.
5. All rays which reach the receiver after a single bounce have the same average power. This is normally reasonable if all the scatterers under consideration are equidistant from the receiver or, if the distance from the scatterers to the receiver is much lesser than the distance between the transmitter and the receiver. Then the difference of average power of different rays is negligibly small.
6. No Line of Sight (LOS) signal is assumed between the transmitter and the receiver.

3.2 Geometrically Based Circular channel model for MIMO systems

In the circular channel model, the mobile is assumed to be surrounded by scatterers which are uniformly distributed in a circle of radius R . The transmitter (generally a

cellular base station) is assumed to be located far away from any scatterers. A schematic representation of this model is given in figure.3.2.1 (Adapted from [Shiu00]).

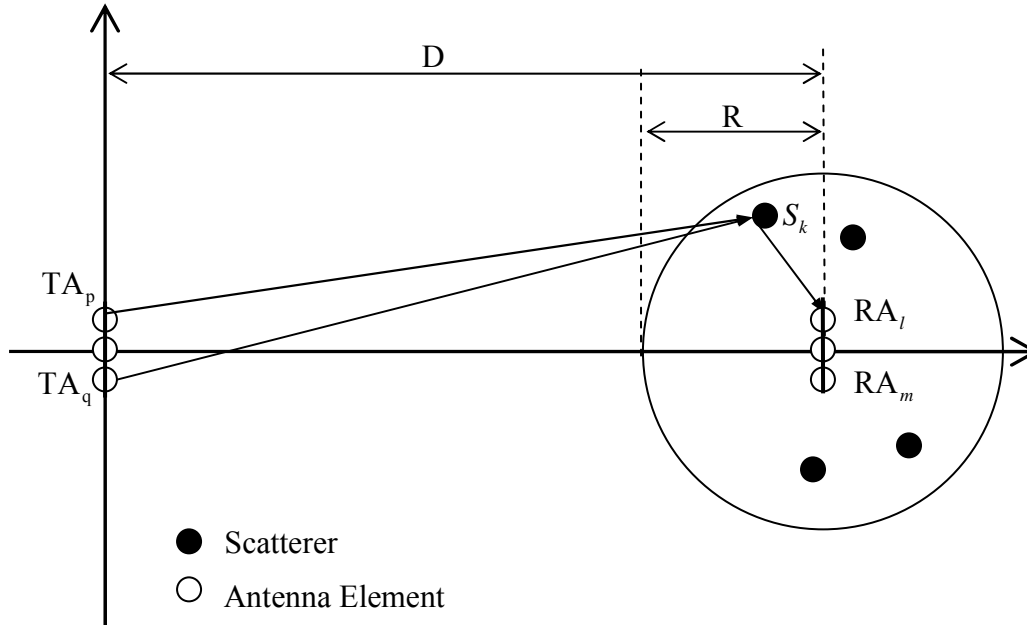


Figure 3.2.1 Geometrically based circular channel model

In the figure

TA_p is antenna element p of the base station array with co-ordinates (x_{tp}, y_{tp})

RA_l is antenna element l of the mobile array with co-ordinates (x_{rl}, y_{rl})

S_k is the k^{th} scatterer with co-ordinates (x_k, y_k)

D is the distance between base station and mobile.

The scatterers are distributed uniformly within a circle of radius R . In order to simulate a flat fading scenario, this radius should be small enough such that the difference in time of arrival (TOA) of rays from various scatterers is lesser than the inverse of symbol rate. (All simulations in this work assume that the radius is adjusted to model flat fading). To model a frequency selective fading channel for CDMA type wideband systems, multiple scatterer clusters can be used. Each cluster should be separated from all others by a

distance large enough to make sure that signals from various clusters can be resolved for a given receiver resolution [Bue01].

For a fixed R , the geometry of the circular channel model is determined by the angle spread Δ . In this case, this is defined as difference between the maximum and minimum possible values of angle of arrival/departure. As all the scatterers are within a circle, the spread in angle of arrival/departure of signals at the base station is dependant on D and R .

$$\Delta_b = 2Tan^{-1}\left(\frac{R}{D}\right), \quad (3.1)$$

where Δ_b indicates that we are considering the angle spread at the base station. At the mobile the angle spread would be 2π as scattered rays can arrive from all angles. The mean angle of arrival/departure of signals at the base station Θ (usually measured with respect to array broadside) also affects the fading at various antenna base station elements. It was shown in [Lee73] that correlation between various antenna elements increases as Θ approaches 90° . (In figure 3.2.1 Θ is assumed to be zero)

The normalized effective path gain between antenna element p of the base station and antenna element l of the mobile can be given as

$$H_{l,p} = \frac{1}{\sqrt{K}} \sum_{k=1}^K \exp \left[-j \frac{2\pi}{\lambda} (D_{TA_p \rightarrow S_k} + D_{S_k \rightarrow RA_l}) + j\phi_k \right]. \quad (3.2)$$

In (3.2)

$$D_{TA_p \rightarrow S_k} = \sqrt{(x_{tp} - x_k)^2 + (y_{tp} - y_k)^2} \quad (3.3)$$

is the distance between base station antenna element p and k^{th} scatterer,

$$D_{S_k \rightarrow RA_l} = \sqrt{(x_{rl} - x_k)^2 + (y_{rl} - y_k)^2} \quad (3.4)$$

is the distance between mobile antenna element l and k^{th} scatterer.

K is the total number of scatterers considered and ϕ_k is the random phase associated with scatterer k .

Using Central limit theorem, if a large number of scatterers are present, the distribution of $H_{l,p}$ approaches that of a zero mean complex Gaussian random variable with variance 0.5 per real dimension (Rayleigh fading). The $n_T \times n_R$ channel matrix H is constructed by using (3.2) for computing path gains between all the transmit and receive antenna elements.

$$H = \begin{bmatrix} H_{1,1} & H_{1,2} & \cdots & H_{1,n_T} \\ H_{2,1} & H_{2,2} & \cdots & H_{2,n_T} \\ \vdots & & & \\ H_{n_R,1} & H_{n_R,2} & \cdots & H_{n_R,n_T} \end{bmatrix}. \quad (3.5)$$

n_T is the number of antenna elements in the base station and n_R is the number of elements in the mobile. By stacking all the columns of H one below each other a $n_R n_T \times 1$ vector called $VecH$ is obtained.

$$VecH = [h_1' \quad h_2' \cdots h_{n_T}']', \quad (3.6)$$

where h_i is the i^{th} column of H . (' is used to represent the transpose operator).

The covariance matrix of H can be then defined using $VecH$ as

$$CovH = E[(VecH)(VecH)^\dagger], \quad (3.7)$$

where the expectation is taken over a large number of channel realizations. (\dagger represents the Hermitian operator). The magnitude of complex cross correlation between two different path gains x_1 and x_2 is given by

$$|\rho_{x_1 x_2}| = \left| \frac{E[x_1 x_2^*]}{\sigma_{x_1} \sigma_{x_2}} \right| \quad (3.8)$$

if the mean of both x_1 and x_2 is zero. Thus the Covariance matrix $CovH$ contains necessary information about all the cross-correlations between paths connecting various antenna elements of the base station and the mobile. The effect obtained by changing various parameters of the circular channel model, on the correlation between different antenna elements is illustrated using the following MATLAB examples.

Example 3.2.1: Here a simple scenario is considered where both the Transmitter (Base station) and the Receiver (Mobile) have two antennas each. Hence, $n_R = n_T = 2$. The correlations are affected by four parameters

- 1 The spacing between antenna elements of the transmitter array.
- 2 The spacing between antenna elements of the receiver array.
- 3 The angle spread Δ of the signals at the base station.
- 4 The mean angle of departure of signals at the base station Θ .

In this example the mean angle of departure of all signals from the base station is assumed to be zero ($\Theta = 0$). This means that the receiver is in line with the transmitter array broadside. For each channel realization, scatters are placed in random locations, uniformly distributed within a circle. The radius of this circle is chosen according to the symbol duration to model flat fading. The channel matrix H is computed using (3.2). If

$$H = \begin{bmatrix} h_{11} & h_{12} \\ h_{21} & h_{22} \end{bmatrix} \quad (3.9)$$

where h_{ij} is the path gain between antenna element j of the base station and antenna element i of the mobile. Then, from (3.6)

$$VecH = [h_{11} \quad h_{21} \quad h_{12} \quad h_{22}]' \quad (3.10)$$

and from (3.7)

$$\text{Cov}H = \begin{bmatrix} E[h_{11}h_{11}^*] & E[h_{11}h_{21}^*] & E[h_{11}h_{12}^*] & E[h_{11}h_{22}^*] \\ E[h_{21}h_{11}^*] & E[h_{21}h_{21}^*] & E[h_{21}h_{12}^*] & E[h_{21}h_{22}^*] \\ E[h_{12}h_{11}^*] & E[h_{12}h_{21}^*] & E[h_{12}h_{12}^*] & E[h_{12}h_{22}^*] \\ E[h_{22}h_{11}^*] & E[h_{22}h_{21}^*] & E[h_{22}h_{12}^*] & E[h_{22}h_{22}^*] \end{bmatrix}, \quad (3.11)$$

where the expectation is over a large number of channel realizations. As mentioned earlier, each element in a particular realization of H is a sample of a complex Gaussian random variable with zero mean and unit variance per complex dimension. So, the magnitude of cross correlation between two different paths h_{lp} and h_{mq} is

$$|\rho_{h_{lp}h_{mq}}| = \left| E[h_{lp}h_{mq}^*] \right|, \quad (3.12)$$

which is the magnitude of the elements of the covariance matrix. Figure 3.2.2 illustrates the covariance matrix of the channel, for various transmit antenna element separations. In all cases, spacing between various receive antenna elements is assumed to be $\lambda/2$, where λ is the carrier wavelength (taken as 0.157m in all simulations). Fig 3.2.2a identifies various paths of the MIMO channel and the correlations between them. Fig. 3.2.2b shows the arrangement of various elements in the covariance matrix plots. Figs 3.2.2c to 3.2.2f show the covariance matrices generated by varying the transmit antenna spacing from 0.5λ to 20λ .

It can be seen from these figures that correlation between paths from two different transmit antennas to the same receive antenna decreases as the transmit element spacing increases. The correlation between receive elements however is constant at a relatively lower value as the receive element spacing is maintained constant. This effect is also shown in Figure 3.2.3.

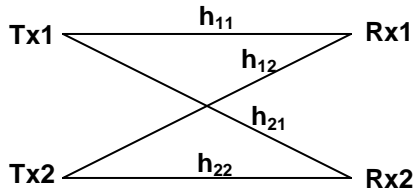


Fig. 3.2.2a

$ \rho_{22,11} $	$ \rho_{22,21} $	$ \rho_{22,12} $	$ \rho_{22,22} $
$ \rho_{12,11} $	$ \rho_{12,21} $	$ \rho_{12,12} $	$ \rho_{12,22} $
$ \rho_{21,11} $	$ \rho_{21,21} $	$ \rho_{21,12} $	$ \rho_{21,22} $
$ \rho_{11,11} $	$ \rho_{11,21} $	$ \rho_{11,12} $	$ \rho_{11,22} $

Fig. 3.2.2b

Circular model, Tx spacing = 0.5λ, Rx spacing = 0.5λ, Δ = 5degrees

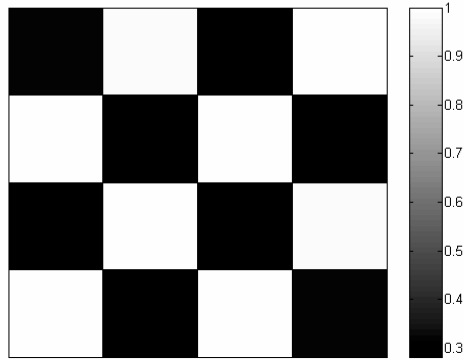


Fig. 3.2.2c

Circular model, Tx spacing = 5λ, Rx spacing = 0.5λ, Δ = 5degrees

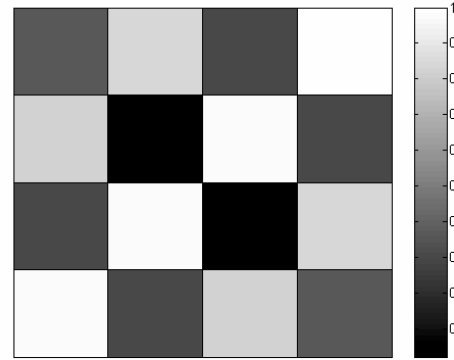


Fig. 3.2.2d

Circular model, Tx spacing = 10λ, Rx spacing = 0.5λ, Δ = 5degrees

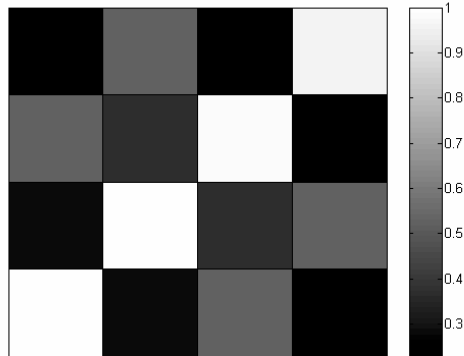


Fig. 3.2.2e

Circular model, Tx spacing = 20λ, Rx spacing = 0.5λ, Δ = 5degrees

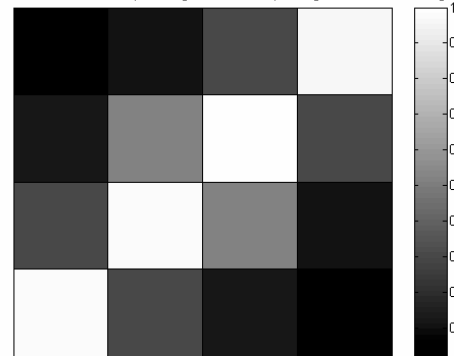


Fig. 3.2.2f

Figure 3.2.2 Covariance Matrix of Circular channel model for various Tx antenna separations. Rx antenna separation is 0.5λ. (λ here is assumed to be 0.15m.)

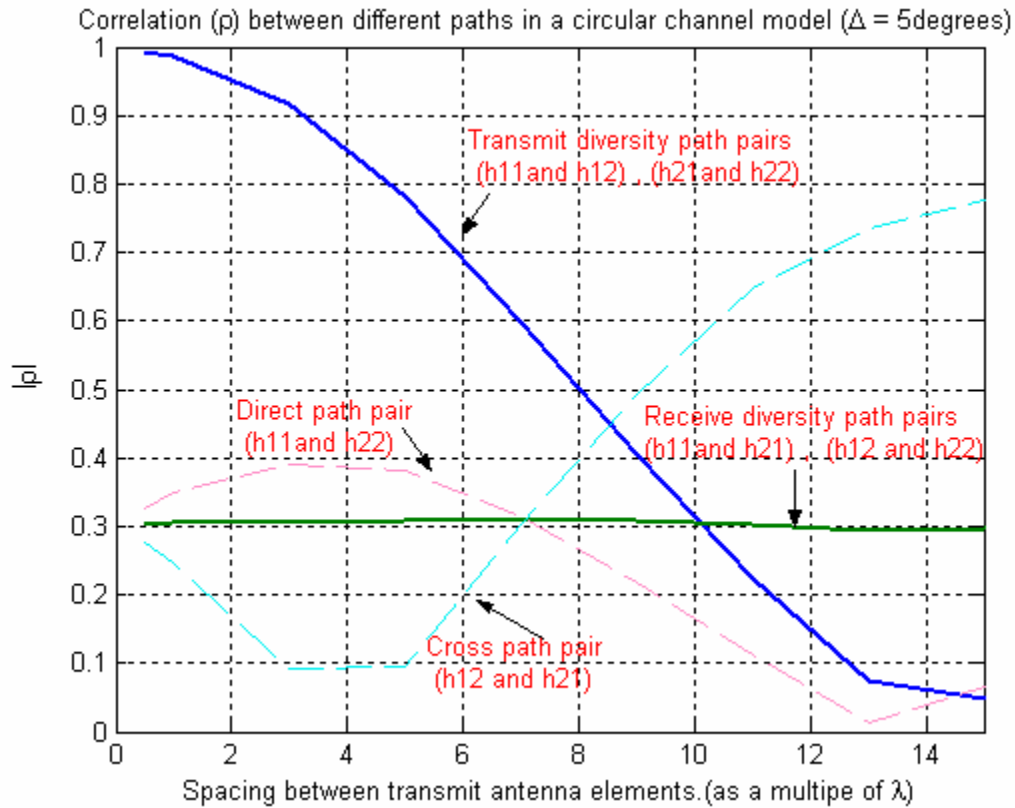


Figure 3.2.3 Variation of correlation with Tx antenna spacing in a circular channel model

Fig. 3.2.4 illustrates the dependence of correlation on the angle spread of signals at the base station. The correlation decreases with increasing angle spread. Two different cases, one with a transmit element spacing of 0.5λ and the other with 10λ , are illustrated in the plot. It can be seen that for a spacing of 10λ , correlation decreases much more rapidly with an increase in angle spread.

Example 3.2.2: A scenario with the transmitter having an eight element uniform linear array and a receiver with single antenna is considered here. The channel matrix, its covariance and the correlation of signals between various paths can be found by employing the procedure used in the previous example.

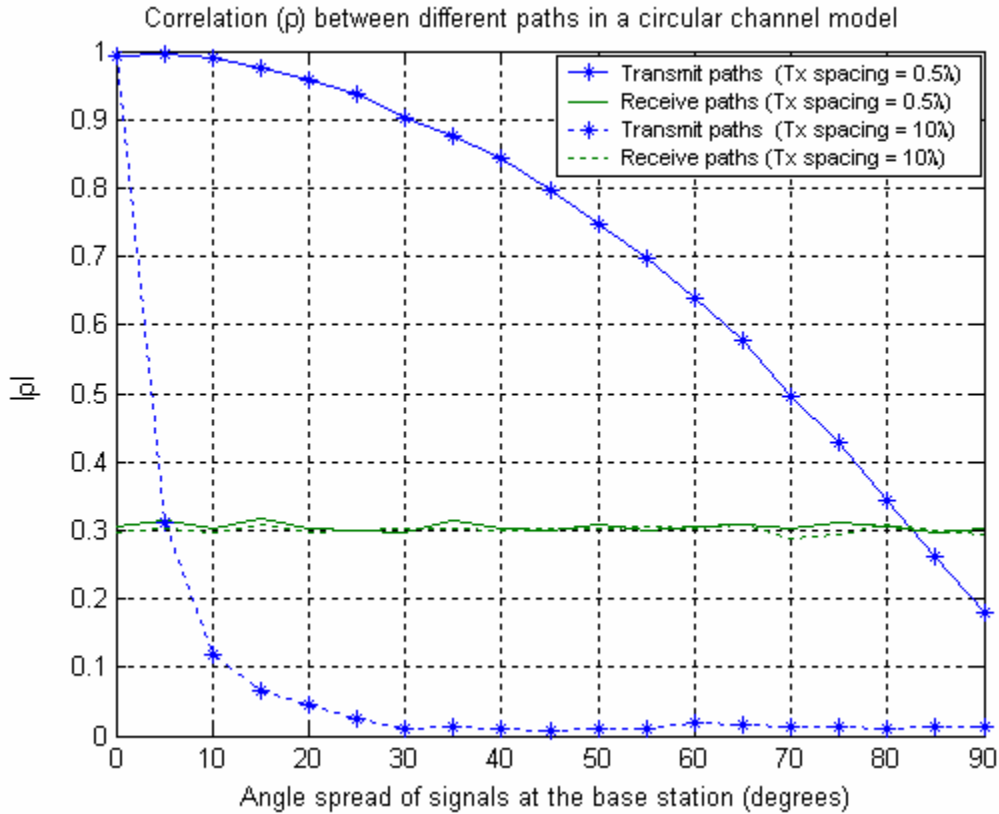


Figure 3.2.4 Variation of correlation with angle spread

Here, there are eight different paths between the transmitter and receiver. For a given geometry and antenna spacing, the correlation between paths starting from any two adjacent transmit antenna elements would be similar. The correlation between paths from non adjacent elements would be lesser. i.e., if the elements of the transmitter array are named 1 through 8, and if the correlation between the elements 1 and 2 is ρ , then the correlation between elements 1 and 3 would be lesser than ρ . Figure 3.2.5 shows the correlation of elements 2 to 8 with the first antenna element for various values of inter-element spacing. The correlation decreases as we go from element 2 to element 8. The rate of decrease is more rapid when the spacing between antenna elements is increased.

In Chapter 2 and in [Goz02a] it was assumed that correlation between various elements follows a geometric progression $(\rho, \rho^2, \dots, \rho^M)$ and the covariance matrix was

modeled to have a Toeplitz form. Dotted lines in Figure 3.2.5 show how the correlations would be, if they decrease in a geometric progression.

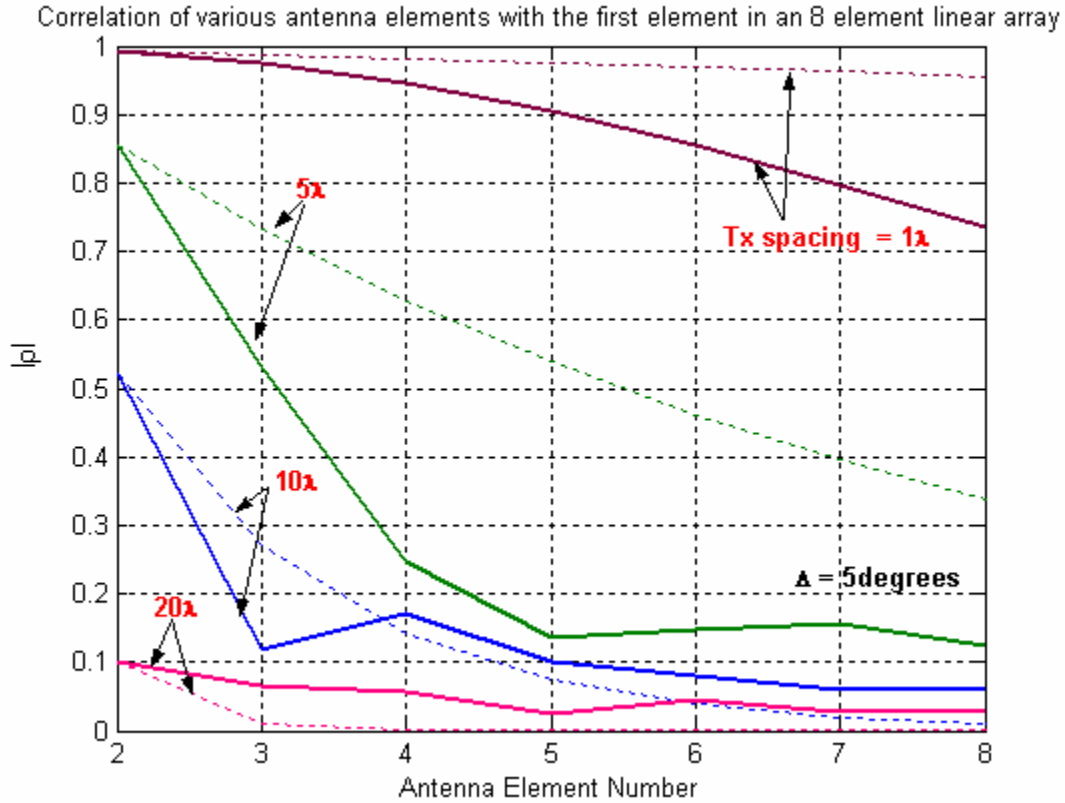


Figure 3.2.5: Correlation of various antenna elements with the first antenna in an 8 element linear array for the circular model (dotted lines show the variation if a Toeplitz structure is used to model the covariance matrix).

3.3 Geometrically Based Elliptical channel model for MIMO systems

In this model both the mobile and base station are assumed to be surrounded by scatterers which lie within an ellipse. Let D be the distance between the transmitter (base station) and the receiver (mobile) and τ_m be the maximum possible propagation delay of any ray arriving at the receiver (considering only those rays which take a single bounce from scatterers). Then, all the scatterers on which the signals may bounce should lie within an ellipse whose semi major axis a_m and the semi minor axis b_m are given by

$$a_m = \frac{c\tau_m}{2}, \quad (3.13)$$

$$b_m = \frac{1}{2}\sqrt{4a_m^2 - D^2}. \quad (3.14)$$

c is the speed of light. Figure 3.3.1 gives a schematic representation of the elliptical channel model.

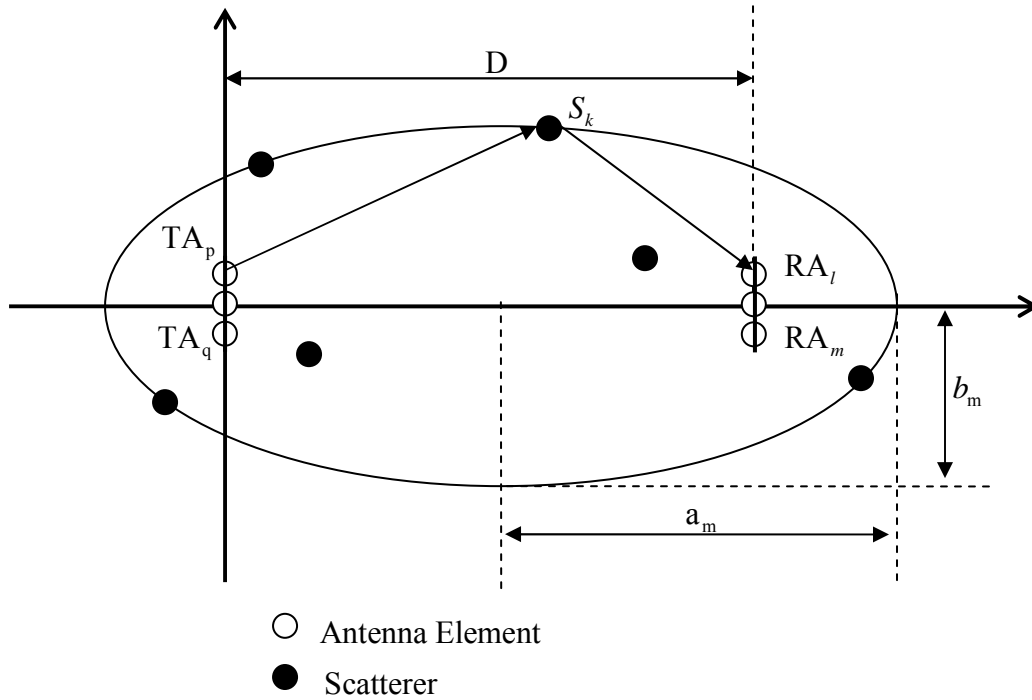


Figure.3.3.1 Geometrically based elliptical channel model

Here,

TA_p is antenna element p of the base station array with co-ordinates (x_p, y_p)

RA_l is antenna element l of the mobile array with co-ordinates (x_{rl}, y_{rl})

S_k is the k^{th} scatterer with co-ordinates (x_k, y_k)

D is the distance between base station and mobile.

a_m is the semi major axis of the ellipse as defined in (3.3.1)

b_m is the semi minor axis of the ellipse as defined in (3.3.2)

The transmitter and receiver are modeled to be located at the two foci of the ellipse, so that its focal length is equal to the transmit - receive distance D . The locus of all points that lie on the ellipse in (Shown in fig. 3.3.1) is given by

$$\frac{\left(x - \frac{D}{2}\right)^2}{a_m^2} + \frac{y^2}{b_m^2} = 1. \quad (3.15)$$

Using (3.14) , (3.15) can be written as

$$\frac{\left(x - \frac{D}{2}\right)^2}{a_m^2} + \frac{y^2}{\frac{1}{4}(4a_m^2 - D^2)} = 1. \quad (3.16)$$

It can be seen from (3.13) and (3.16) that the two parameters which determine the geometry of the ellipse are the maximum allowable delay τ_m and the transmit receive distance D . For (3.16) to be an equation of a valid ellipse,

$$a_m > \frac{D}{2}. \quad (3.17)$$

Note that $a_m = 0.5D \Rightarrow b_m = 0$ and the ellipse collapses into a straight line.

Therefore ,using (3.17) and (3.13)

$$\tau_m > \tau_0, \text{ where } \tau_0 = \frac{D}{c}. \quad (3.18)$$

τ_m can be represented as

$$\tau_m = \tau_0 + \Delta\tau_m, \quad (3.19)$$

where $\Delta\tau_m$ is the maximum possible difference in the Time Of Arrival (TOA) of the rays at the receiver. Using (3.18) and (3.13)

$$a_m = \frac{D}{2} + \frac{c(\Delta\tau_m)}{2}. \quad (3.20)$$

In a flat fading scenario the maximum difference in TOA of signals arriving at the receiver should be less than the inverse of symbol rate, denoted here by $\Delta\tau_r$. (This means that the receiver cannot resolve the rays whose difference in TOA is $\Delta\tau_r$ or less). Hence, in order have an ellipse which model's flat fading

$$\Delta\tau_m \leq \Delta\tau_r. \quad (3.21)$$

Therefore, to model a flat fading scenario the major axis of the ellipse should satisfy the following condition,

$$\frac{D}{2} < a_{mflat} \leq \frac{D}{2} + \frac{c(\Delta\tau_r)}{2}, \quad (3.22)$$

where (3.22) is obtained from (3.17), (3.20) and (3.21). To model a frequency selective fading channel for CDMA type wideband systems scatterers can be placed within elliptical bands whose width is determined by the resolution of the receiver [Lu97].

Only the flat fading scenario is considered for all further analysis. In that case, equations (3.2) to (3.12) which were used for computing the path gains, the channel matrix and the correlations between various antenna elements in the circular channel model are also valid for the elliptical channel model. As in Section 3.2 the effect obtained by changing various parameters of the elliptical channel model, on the correlation between different antenna elements is illustrated in the following MATLAB example.

Example 3.3.1: Similar to Example 3.2.1 a simple scenario where both the Transmitter (Base station) and the Receiver (Mobile) have two antennas each ($n_R = n_T = 2$) is considered. The correlations are affected by

1. Separation between transmit antenna elements.

2. Separation between receive antenna elements.
3. Geometry of the ellipse. (If $\Delta\tau_r$ is fixed, this depends on the transmit-receive distance D).

In this example $\Delta\tau_r$ is fixed at the value $0.52\mu s$. If all the scatterer locations which cause the reflected rays to arrive within this resolution are considered, the semi-major axis of the ellipse would be (using 3.3.9),

$$a_{mflat} = \frac{D}{2} + \frac{c(0.52\mu s)}{2} = 0.5D + 78m. \quad (3.23)$$

The semi minor axis can be obtained using (3.22) in (3.14). For each channel realization, scatterers are placed in random locations, uniformly distributed within this ellipse. The structure channel matrix H and its covariance $CovH$ for this model would be the same as those in Example 3.2.1. The correlation between different antenna elements can also be measured in the same way as in Example 3.2.1.

Figure 3.3.2 illustrates the covariance matrix of elliptical channel model for various values of separation between transmit antenna elements. The receive antennas are assumed to be separated half wavelength apart in all the cases. Transmit receive distance D is set at 1000m. Fig 3.3.2a identifies various paths of the MIMO channel and the correlations between them. Fig. 3.3.3b shows the arrangement of various elements in the covariance matrix plots. Figs 3.3.3c and 3.3.2d show the covariance matrices generated for of transmit antenna spacing of 0.5λ and 5λ respectively.

It is evident from that plots that in the presence of scatterers around both the transmitter and the receiver, the correlation between various paths in the MIMO model is much lower. This effect is also illustrated in Figure 3.3.3. Here the magnitude of correlation between various paths is plotted for transmit spacing ranging from 0.5λ to 5λ .

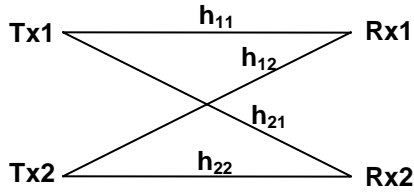


Fig. 3.3.3a

$ \rho_{22,11} $	$ \rho_{22,21} $	$ \rho_{22,12} $	$ \rho_{22,22} $
$ \rho_{12,11} $	$ \rho_{12,21} $	$ \rho_{12,12} $	$ \rho_{12,22} $
$ \rho_{21,11} $	$ \rho_{21,21} $	$ \rho_{21,12} $	$ \rho_{21,22} $
$ \rho_{11,11} $	$ \rho_{11,21} $	$ \rho_{11,12} $	$ \rho_{11,22} $

Fig. 3.3.3b

Elliptical Model Tx spacing = 0.5λ , Rx spacing = 0.5λ , D = 1000m

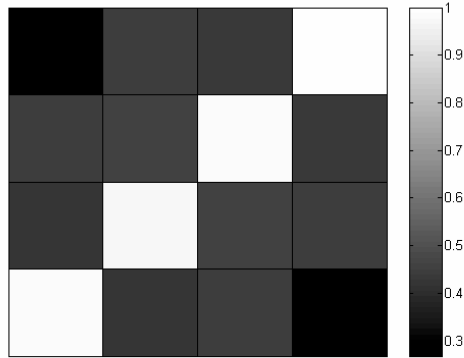


Fig. 3.3.3c

Elliptical Model Tx spacing = 5λ , Rx spacing = 0.5λ , D = 1000m

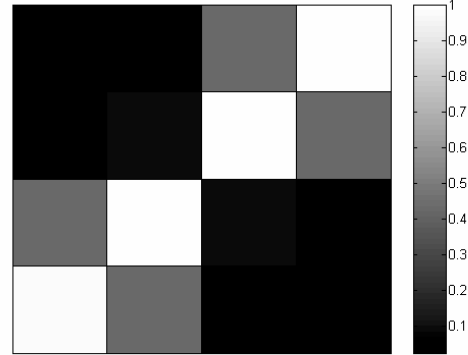


Fig. 3.3.3d

Figure 3.3.2 Covariance Matrix of Elliptical channel model for various Tx antenna separations. Rx antenna separation is 0.5λ . (λ here is assumed to be 0.15m.)

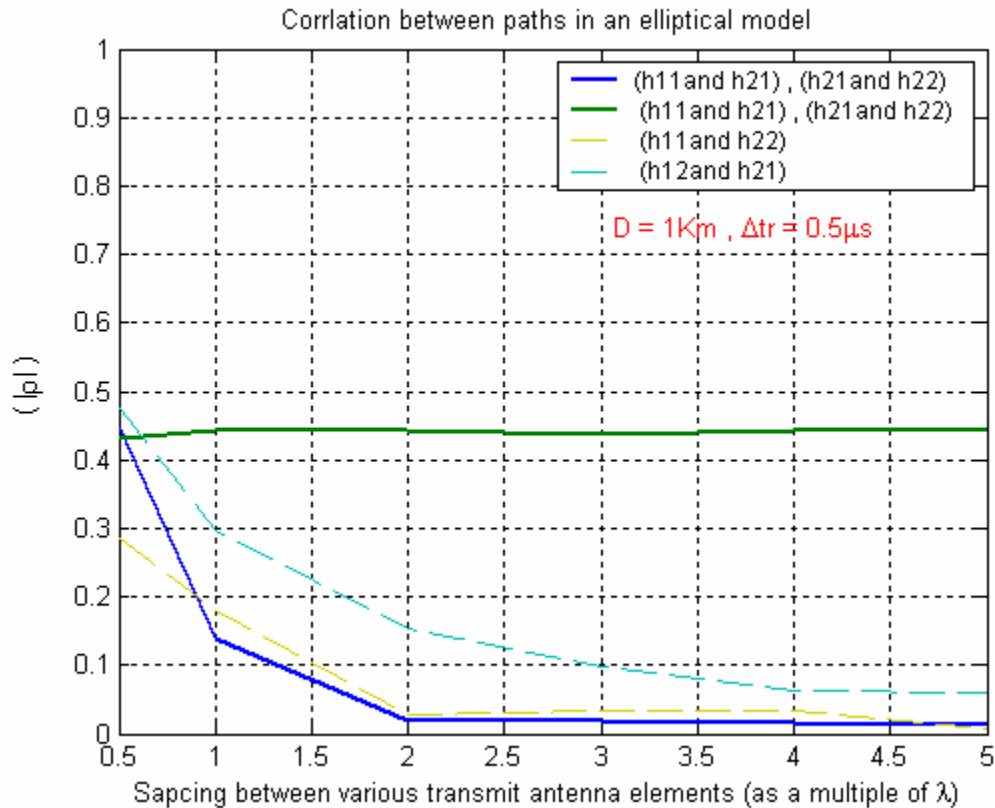


Figure 3.3.3 Variation of correlation with Tx antenna spacing in an elliptical channel model

Different ellipses which model flat fading for $\Delta\tau_r = 0.52\mu\text{s}$ are shown in Figure 3.3.4. These ellipses are obtained for different values of transmit receive distance beginning at 500m. (at distances closer than this, usually the no line of sight assumption may not be valid). As both the transmitter and receiver are surrounded by scatterers, reflected rays can arrive/depart at all possible angles. However as the transmit-receive distance increases, there would be more rays whose angle of arrival/departure is closer to that of line of sight. This effect is shown in figure 3.3.5.

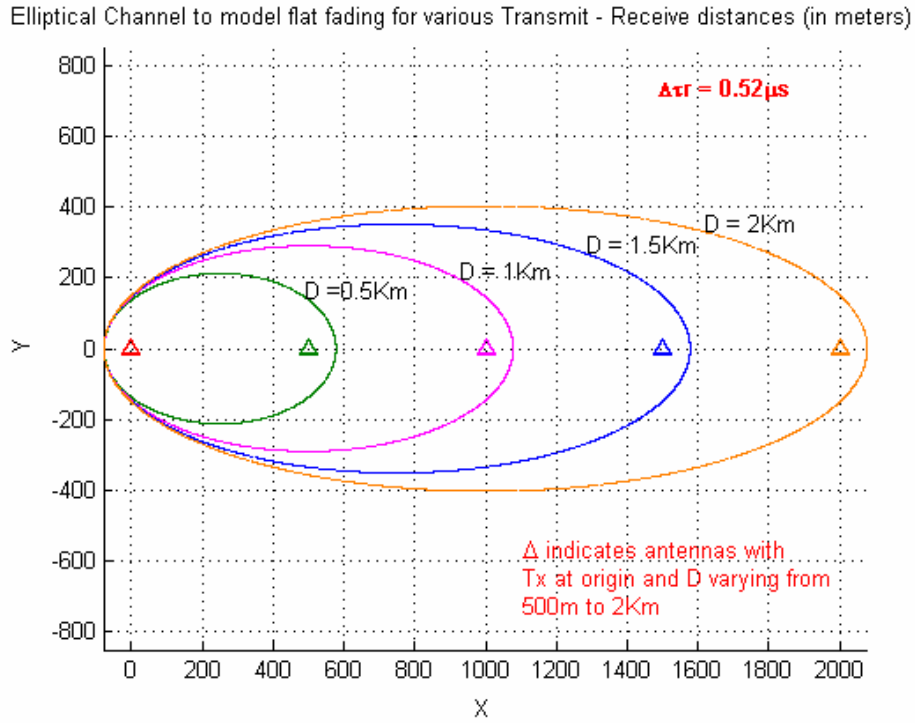


Figure 3.3.4 Ellipses in which uniformly distributed scatterers cause flat fading. (different colors show different transmit distances)

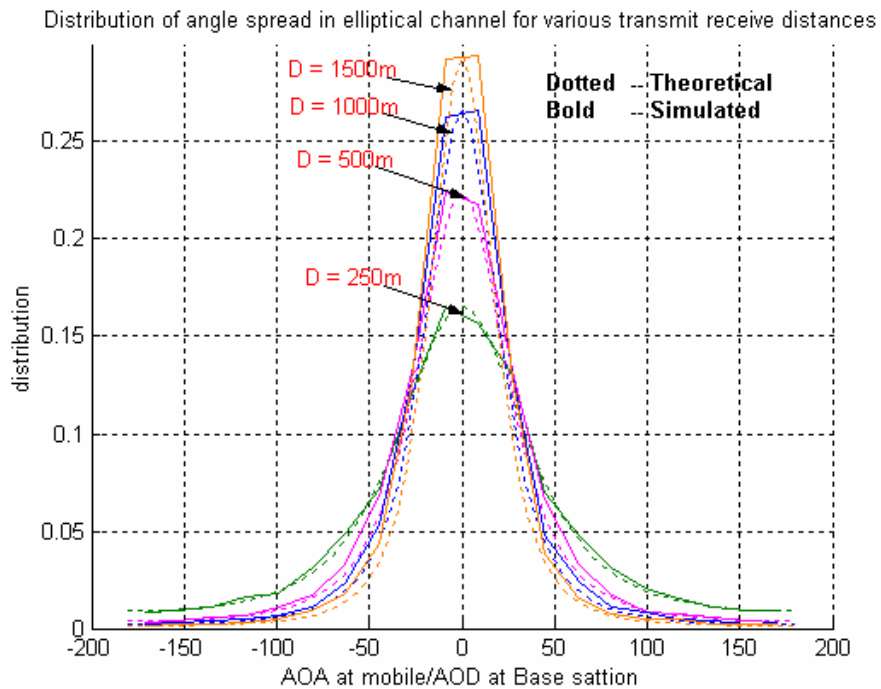


Figure 3.3.5 Distribution of angle spread in an elliptical channel for various transmit receive distances

As the angle spread distribution gets narrower the correlation between signals from the different transmit antennas increases. The same effect is also observed for signals at the receive antennas. This is illustrated in Figure 3.3.6

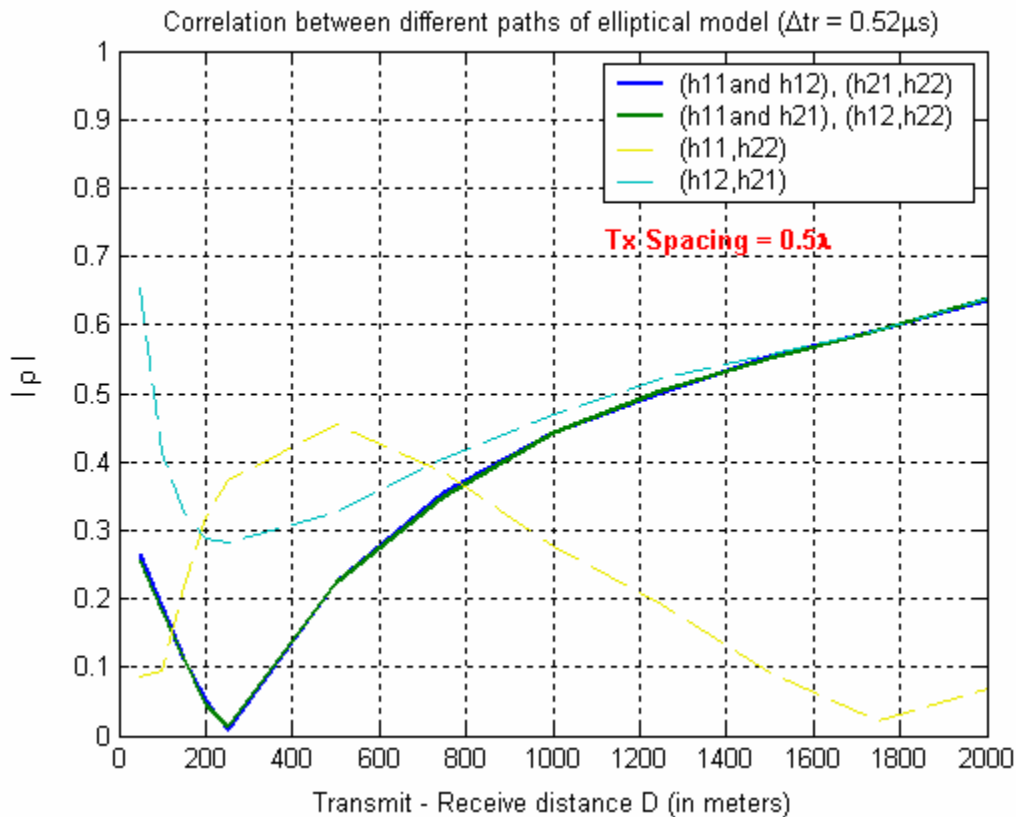


Figure 3.3.6: Variation of correlation with Transmit – Receive distance in an elliptical channel model

3.4 Performance of STBC in GBSB-MIMO models

Using the analysis described in the previous two sections, various channel realizations can be generated for both the circular and elliptical models. These channels can be used for studying the performance of MIMO schemes. In this section, results which characterize the performance of various Space Time Block Coding schemes in GBSB channel models are presented.

In all the channel models, signals at any particular receive antenna are the sum of transmit rays which get reflected by scatterers. If the number of scattered rays arriving at the receiver is reasonably large, then their sum approaches a complex Gaussian distribution and the characteristics of each individual link between the transmit and receive antenna elements approach that of a Rayleigh fading channel. So, the fading characteristics over each individual path¹ in these channel models are similar to those assumed in [Tar99]. i.e., the fade coefficients of each path are instances of complex Gaussian random variables with zero mean and variance 0.5 per real dimension. However the correlation between different paths depends upon the channel model being used and the various parameters associated with it.

3.4.1 Performance of STBC in Circular channel model

The circular model is used to characterize outdoor scenarios. Thus the transmitter would normally be a base station and the receiver would be a cellular handset. In this case the number of elements at the transmitter and the spacing between them is higher than that of the receiver. As discussed in *Example 3.2.1*, the basic parameters which can be varied in the circular model are the spacing between various elements of the transmitter and receiver, the mean angle of arrival of signals and the angle spread. In all the simulations the mean angle of arrival of signals Θ is assumed to be zero and the spacing between receive antenna elements is set as $\lambda/2$ (λ is set as 15cm).

Figure.3.4.1 shows the performance of G2 space time block coding scheme in the circular channel model for a narrow angle spread $\Delta = 5^\circ$. The effect of separation between transmit antenna elements on the BER performance is illustrated here. Results show that for a transmit element spacing less than 5λ there is very little diversity advantage provided by space time block codes and the bit error rates are almost equal to that of single transmit antenna case. As the transmit element spacing is increased the correlation

¹ Here, 'Path' means the channel between a particular transmit-receive antenna pair. This notation will be continued hereafter.

between signals from various transmit paths is decreased and the performance improves due to better diversity advantage. For the 2Tx – 1Rx scenario, bit error rate curves approach the uncorrelated fading scenario when the transmit element spacing greater than 10λ . However for 2Tx – 2Rx case, even with 20λ transmit spacing the performance is slightly worse than that in uncorrelated fading. This is can be attributed the small amount correlation between receive antenna elements (about 0.3 according to predictions in Figure 3.2.3).

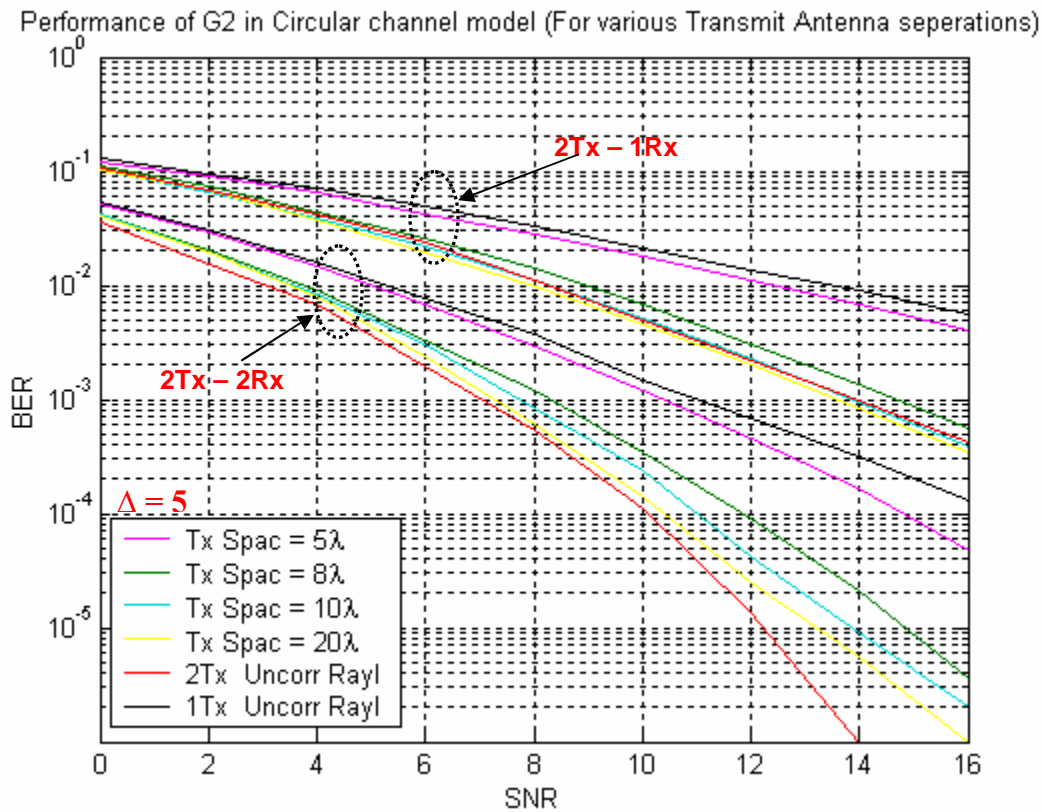


Figure 3.4.1 Performance of G2 – STBC in Circular Channel (Effect of Transmit element spacing)

Figure 3.4.2 (3.4.2(a) for one receive antenna and 3.4.2(b) for two receive antennas) shows the performance of G4 for various values of transmit element spacing. As 4 transmit elements are employed, the performance is better than the G2 case but the dependence on separation between transmit antenna elements follows the same pattern as in Figure 3.4.1.

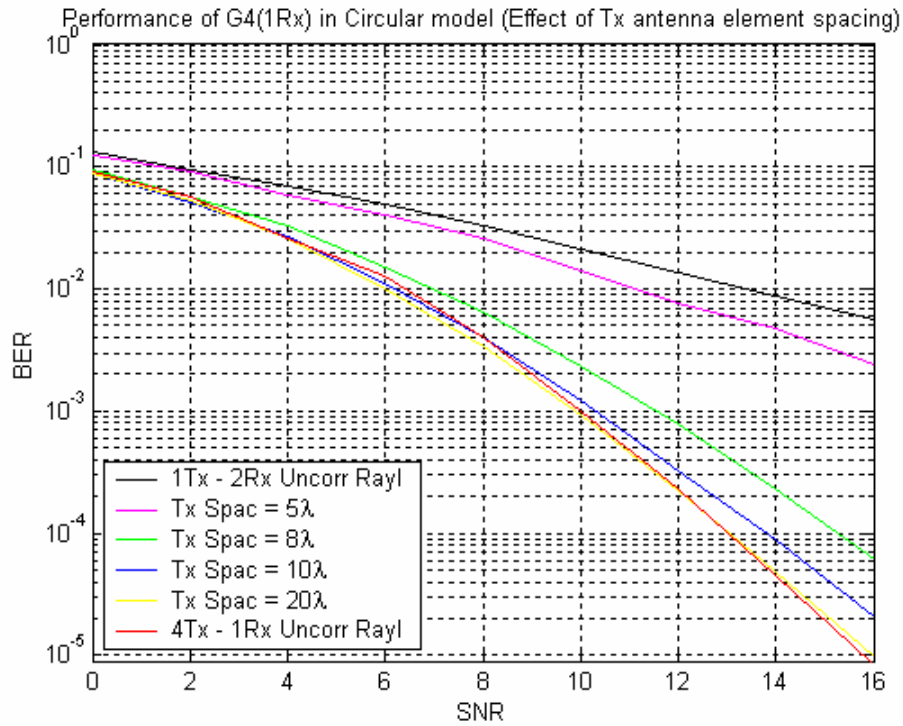


Figure 3.4.2(a) Performance of G4 STBC in Circular model (1Rx antenna)

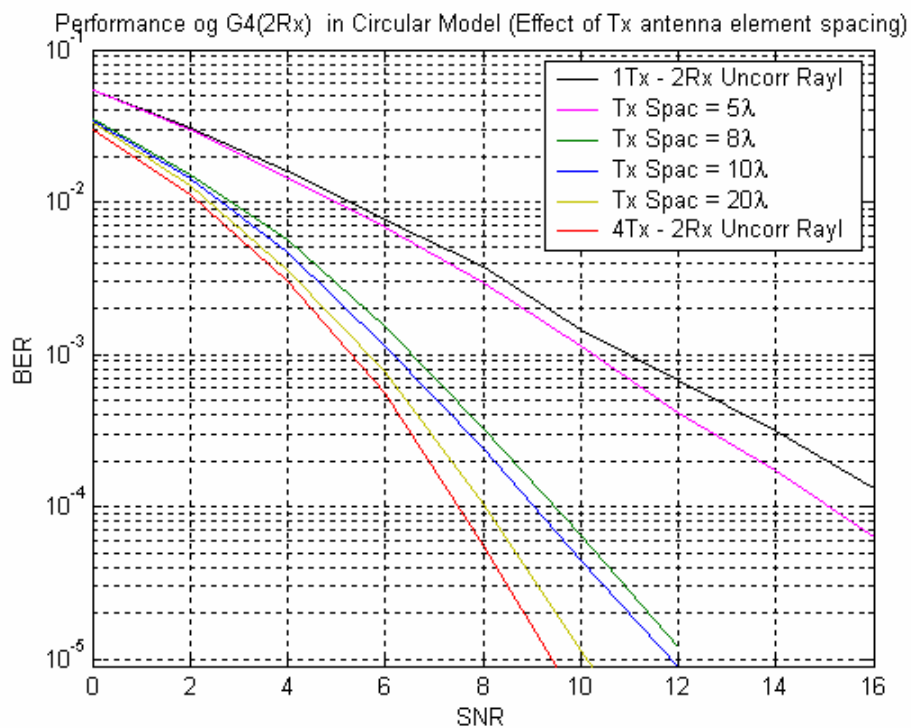


Figure 3.4.2(b) Performance of G4 STBC in Circular model (2 Rx antennas)

The dependence of performance on the angle spread of signals at the base station is illustrated in Figure 3.4.3. Results of two cases, one with a narrow angle spread of 5 degrees and the other with a larger angle spread of 30 degrees are shown. BER curves indicate that if the transmit elements are spaced moderately far apart (5λ), the performance with larger angle spread signals is much better when compared to that of lower angle spreads. This is because, as the angle spread increases the correlation between signals at various transmit antenna elements decreases (Figure 3.2.4).

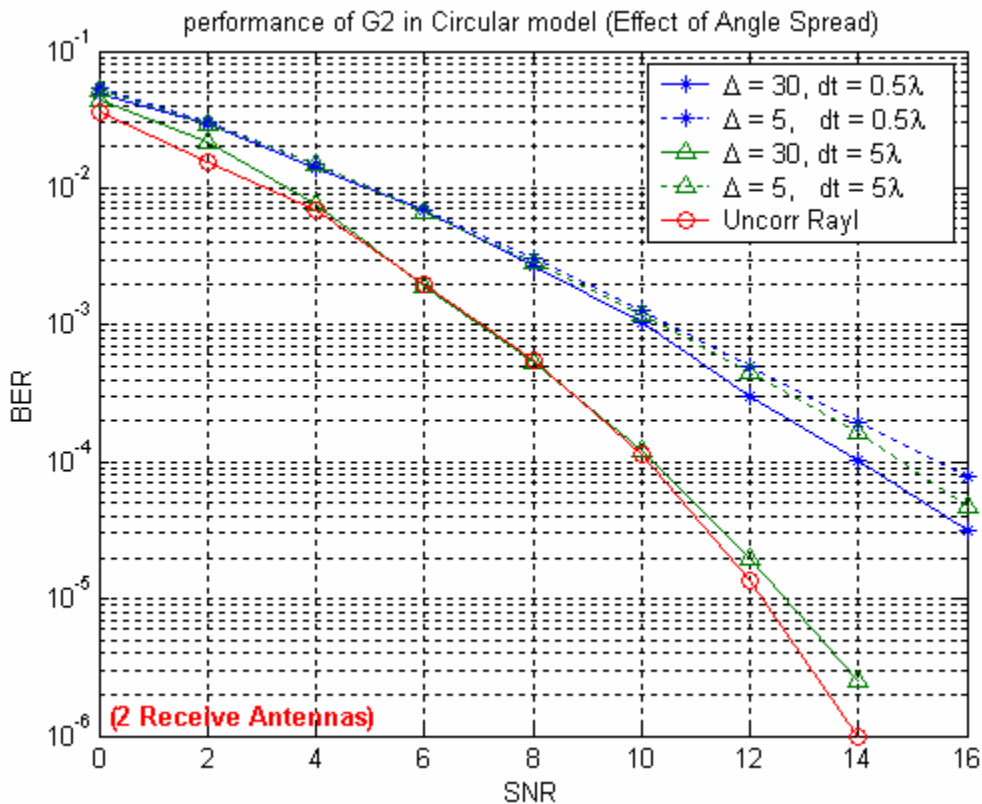


Figure 3.4.3 Effect of Angle Spread on the Performance of G2 STBC in circular model (2Rx Antennas)

3.4.2 Performance of STBC in Elliptical channel model

Signals between various paths in the elliptical channel model are usually less correlated when compared to those in circular channel. This is because in the elliptical model both the transmitter and the receiver are surrounded by scatterers. However the correlation

increases when the geometry of the ellipse (in which the scatterers are present) becomes narrow (Figure 3.3.6). The performance of G2 – STBC scheme in an elliptical channel model is shown in Figure. 3.4.4. Similar to *Example 3.3.1*, the receiver resolution is fixed and the geometry of ellipse is varied by changing its focal length (which is the transmit – receive distance D). BER curves in the figure show that as D increases (the ellipse becomes narrower) the performance degrades due to higher correlation. BER curves indicate that the performance degradation for 2Tx – 2Rx scheme is much more when compared to 2Tx – 1Rx scheme. This effect can be attributed to the presence of additional receive correlation in the 2Tx – 2Rx case. In fact, due to the symmetrical structure of the elliptical model, as the ellipse becomes narrower, the correlation between different paths at both the transmitter and receiver increases equally (Figure 3.3.6).

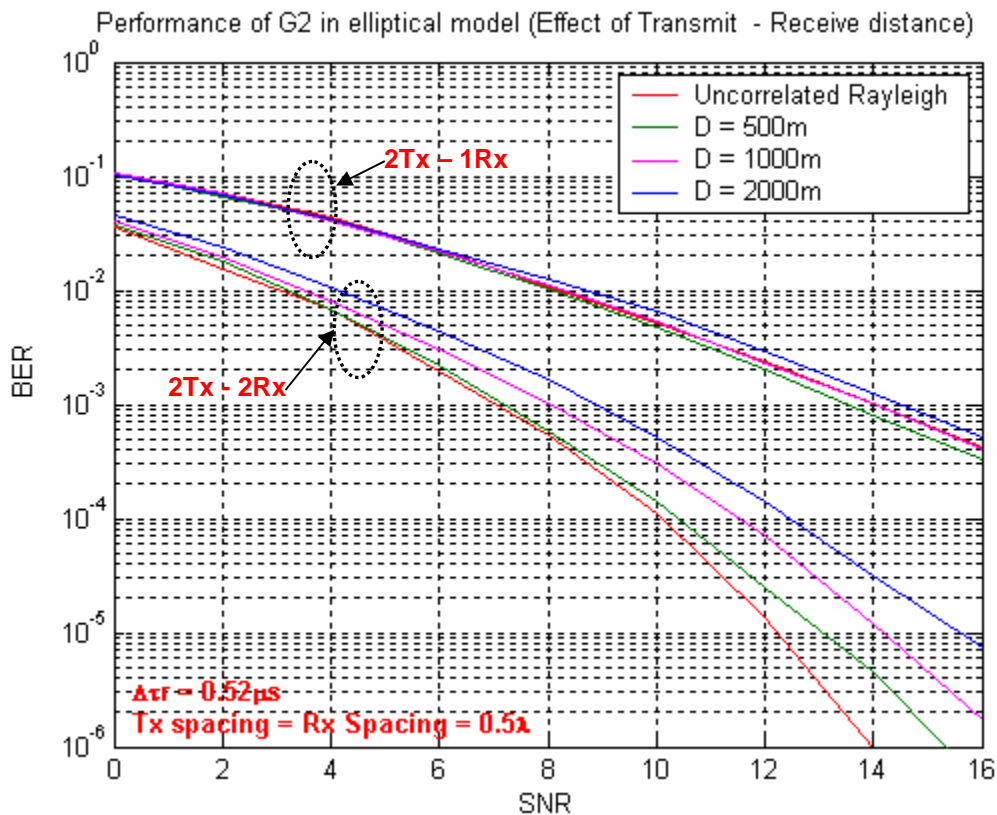


Figure 3.4.4 Performance of G2 STBC in elliptical model (Effect of geometry of ellipse)

Similar results are also observed for G4 – STBC scheme whose performance is illustrated in Figure 3.4.5.

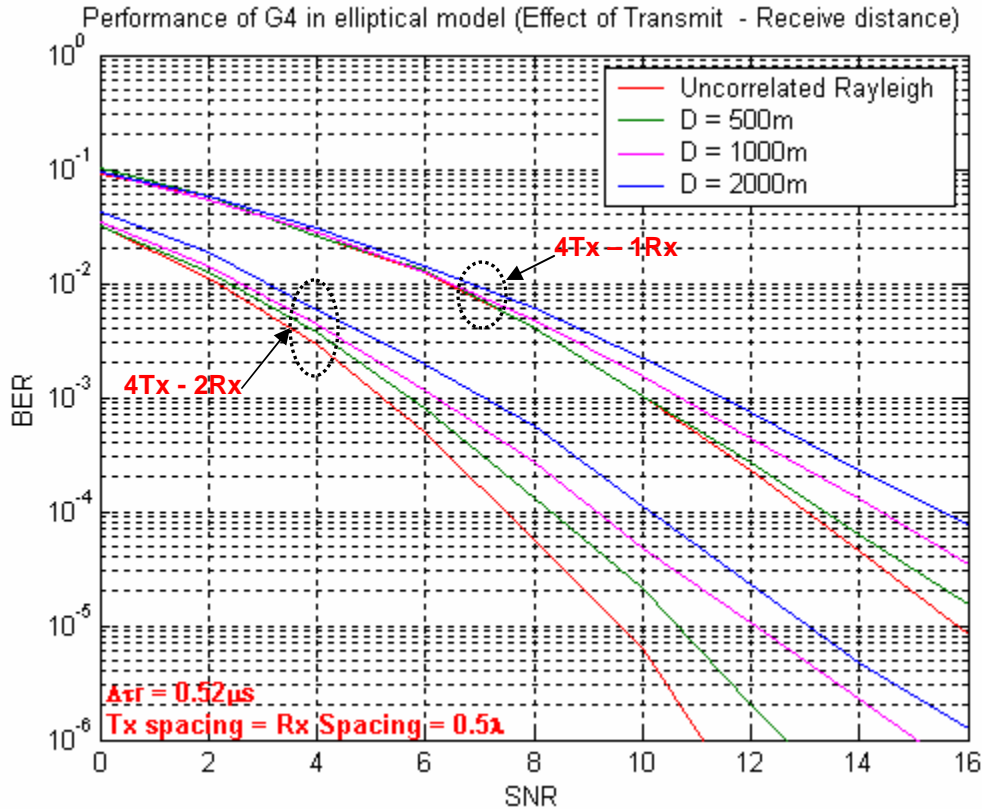


Figure 3.4.5 Performance of G4 STBC in elliptical model (Effect of geometry of ellipse)

3.4.3 Comparison of results with analytic bounds

In [Goz02b] an analytic expression for upper bounds on error probability of various space-time block codes is given (See section 2.2.3 for more details). The expression uses Eigen values of the channel covariance matrix to arrive at upper bounds on error probability. In case of GBSB models, if a large number of realizations of the channel matrix H are available, the covariance matrix can be obtained using (3.11). This matrix can be used in the analytic expression to arrive at theoretical upper bounds on STBC error performance for in various channel models. Plots comparing these upper bounds and the results obtained in the previous sections are shown in Figures 3.4.6 and 3.4.7. It can be seen from the figures that the results obtained from Monte Carlo simulations match closely with the upper bounds computed by using the channel covariance matrices.

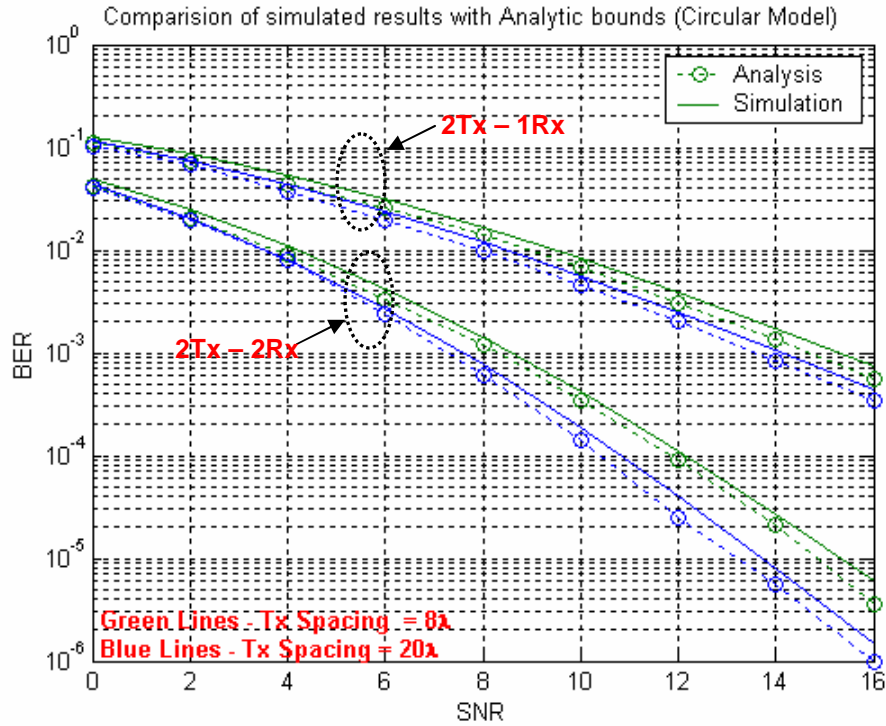


Figure 3.4.6(a) Comparison of Analytic and Simulated results for G2 STBC in circular channel

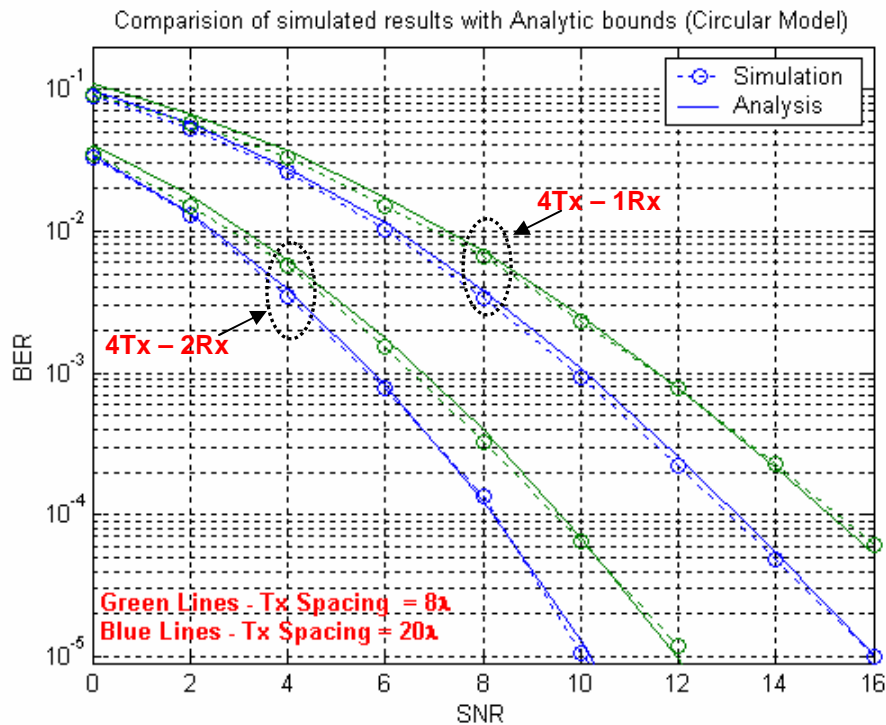


Figure 3.4.6(b) Comparison of Analytic and Simulated results for G4 STBC in circular channel

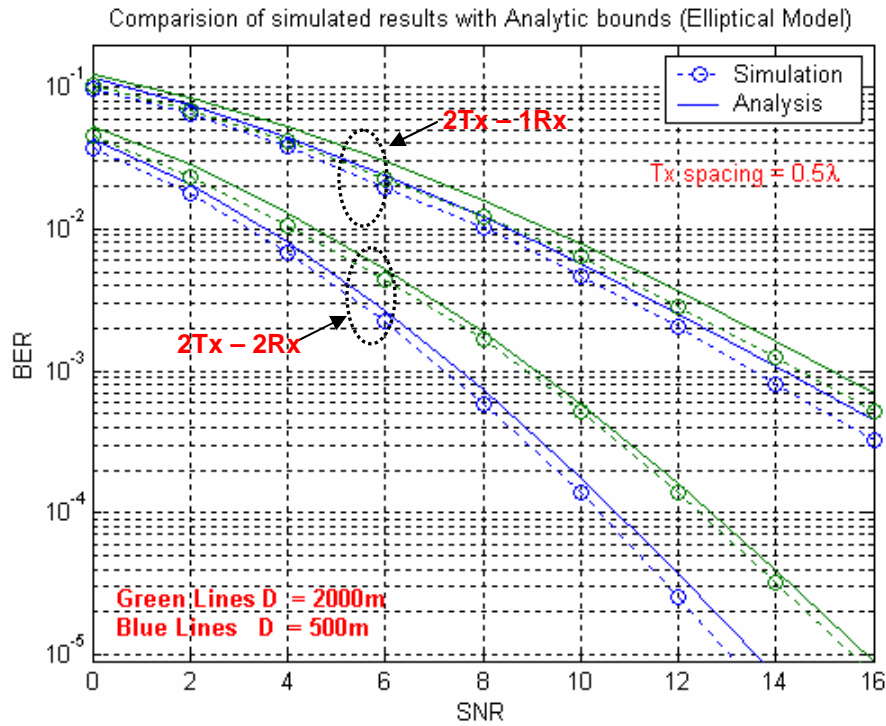


Figure 3.4.7(a) Comparison of Analytic and Simulated results for G2 STBC in elliptical channel

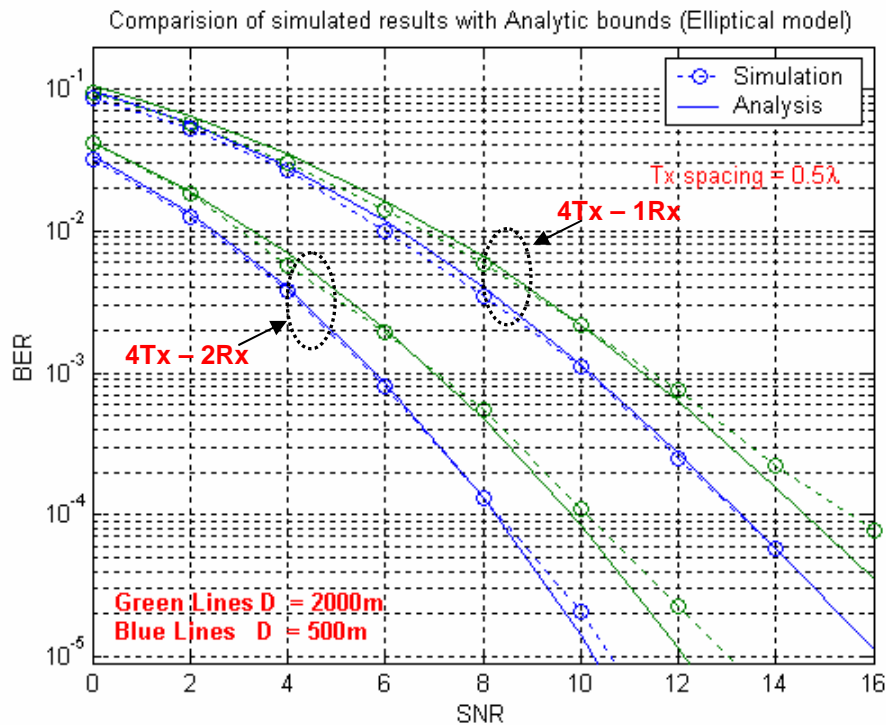


Figure 3.4.7(b) Comparison of Analytic and Simulated results for G4 STBC in elliptical channel

3.5 Summary

In this chapter, the performance of space time block codes was characterized for outdoor scenarios. In order to simulate outdoor environments, two geometrically based vector channel models, one without scatterers around the transmitter and the other with scatterers around the transmitter were considered and procedures to simulate these models were explained. Results show that the fading correlation between various paths in the MIMO system is dependent on the spacing between antenna elements of the transmit and receive arrays and also on the geometry of distribution of scatterers. Performance plots for space-time block coding in these channels indicate a relatively small degradation for low to medium values of correlation and a loss of diversity order for high values of correlation.

Chapter 4

Array Processing with Space-Time Block Codes

Channel state information is usually required for decoding non-differential space time block coding schemes. Thus, the receivers for these schemes need to estimate the amplitude and phase distortion caused by the wireless environment on paths between each transmit and receive antenna element. If multiple receive antenna elements are available, this channel state information can also be used for array processing in conjunction with the space time decoding. A scheme which combines space-time coding with array processing at the receiver was initially presented in [Tar99b]. The authors name this scheme as ‘multi-layered space-time coded modulation’. Here, individual antenna elements of the transmitter are partitioned into small groups and information is transmitted by using a separate space-time code for each group. At the receiver, each individual space-time code is decoded by a layered approach where signals from other groups of antennas are suppressed using array processing. This approach generalizes the layered space time architecture proposed by Foschini in which signals at each antenna are coded individually [Fos96] (This scheme is known as ‘diagonal BLAST’ or D-BLAST). The V-BLAST (vertical BLAST) scheme [Wol98] also uses array processing at the receiver to suppress signals from other antennas, but here signals from each antenna element are uncoded.

In [Jon02] a scheme which combines space-time block coding with array processing at the transmitter is presented. Here the authors propose a method which combines transmit

beamforming with space-time block coding. In order to implement this method the transmitter needs to have estimates of channel parameters of the forward link

The primary advantage of using space-time block codes in a MIMO system is that they utilize the available spatial diversity to provide good error performance at the receiver at low SNR with very little complexity of decoding. However, they don't provide any significant gain in spectral efficiency γ_s . For example, a G2 space-time block code with two receive antennas and M-ary PSK modulation has a spectral efficiency (assuming optimum pulse shaping) of $\gamma_{s(STBC)} = M$ bps/Hz, while an uncoded BLAST scheme with the same number of antennas would provide a spectral efficiency of $\gamma_{s(BLAST)} = 2M$ bps/Hz. In fact if the number of transmit antennas increases to $n_T > 2$, the spectral efficiency of the appropriate STBC scheme would be less than M bps/Hz while the spectral efficiency of BLAST increases to $n_T * M$ bps/Hz (Provided at least n_T receive antennas are available). This is because for $n_T > 2$, the code rate r of the available Space-Time block codes is less than 1. BLAST schemes on the other hand provide high spectral efficiencies at the cost of power efficiency. To achieve the large spectral efficiencies provided by BLAST at a reasonable BER, the required E_b / N_o at the receiver is very high.

This chapter investigates various methods which combine space-time coding with array processing. The basic principles of 'multilayered space-time coded modulation' given in [Tar99b] are applied here with space-time block codes to arrive at schemes which can provide reasonably high spectral efficiencies at a reasonably low SNR. The idea behind these schemes is to use transmit diversity (in the form of Space-Time Block coded transmissions) to improve the power efficiency of BLAST without a considerable loss in its spectral efficiency. Finally, this chapter also presents a discussion on the various issues involved in combining beamforming and space-time coding at the transmitter.

The chapter is organized in the following manner. Section 4.1 gives a brief introduction to the BLAST (BLAST in this chapter refers to the V-BLAST scheme) and studies its

performance in correlated fading. Section 4.2 describes the fundamentals of multilayered space-time coded modulation. Section 4.3 gives details about schemes which use Space-Time Block codes to improve the power efficiency of BLAST. Section 4.4 presents a discussion on transmit beamforming and space-time Block coding. Section 4.5 gives a short summary of the work presented in this chapter.

4.1 Performance analysis of BLAST

BLAST or Bell Labs Layered Space-Time architecture was first proposed by Foschini [Fos96] with the objective of realizing the capacity predictions made by information theoretic analysis of MIMO channels (the analysis is summarized in [Fos98]). Later in Wolniansky, *et. al.* [Wol98], the authors proposed a modified scheme which was more practically realizable. This was called vertical BLAST or V-BLAST. (see Figure 4.1.1).

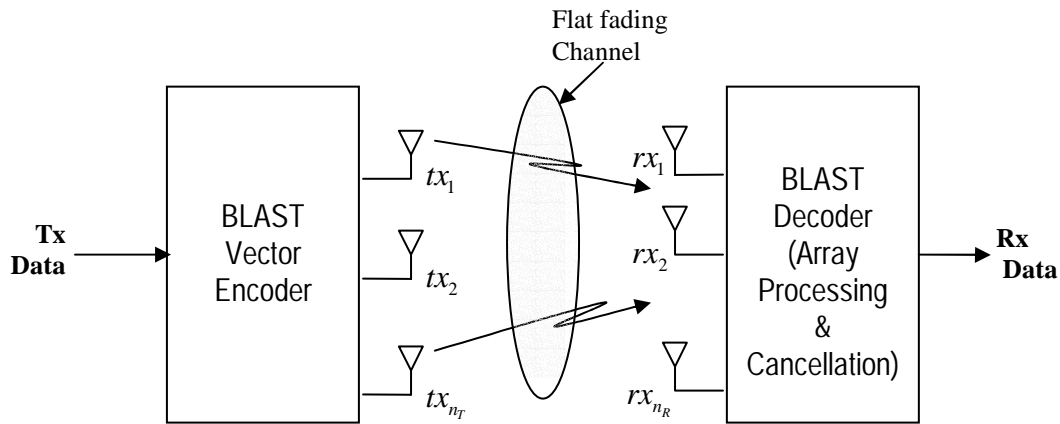


Figure 4.1.1 V-BLAST Scheme

In the V-BLAST scheme (which is referred to as BLAST for the remaining portion of this chapter) information symbols are mapped in parallel streams and each stream is transmitted from a separate transmitter element. If there are a sufficiently large number of scatterers in the channel, and the antenna spacing is reasonably large, then the fading across paths from each transmit to receive antenna will be independent. The channel

delay spread is assumed to be small enough to cause flat fading on the signals transmitted from various antennas. If there are n_T transmit antennas and n_R receive antennas (with $n_R \geq n_T$), the received signal at any particular time can be given as

$$\bar{r}^{(1)} = H\bar{a} + \bar{\eta} \quad (0.1)$$

Where, $\bar{r}^{(1)}$ is a $n_R \times 1$ vector whose elements represent the received signal at each receiver antenna element, H is a $n_R \times n_T$ channel matrix representing MIMO quasistatic flat Rayleigh fading channel between the transmitter and the receiver. \bar{a} is the $n_T \times 1$ vector of transmit symbols and $\bar{\eta}$ is a $n_R \times 1$ noise vector of independent AWGN samples.

As the name suggests, decoding is done using a layered approach. To decode the transmitted symbols of the first layer, the receiver initially estimates the channel matrix H using pilots (perfect channel estimation is assumed in the further analysis). It then considers symbols from a particular transmit antenna as desired signal and suppresses signals from other antennas using array processing. Minimum Mean Squared Error (MMSE) or Zero Forcing (ZF) criteria can be employed for this purpose. If ZF criterion is used to decode symbols from transmit antenna j and suppress signals from all other antennas, the receiver multiplies vector $\bar{r}^{(1)}$ with a $1 \times n_R$ weight vector given by

$$\bar{w}_j = (H^+)_j, \quad (0.2)$$

where $(H^+)_j$ is the j^{th} row of pseudo inverse of matrix H which is given by $H^+ = (H^\dagger H)^{-1} H^\dagger$. If the MMSE criterion is used for suppression then the weight vector would be given by [Bar00]

$$\bar{w}_j = \left(\left[H^\dagger H + \frac{\sigma_n^2}{\sigma_d^2} I \right]^{-1} H^\dagger \right)_j, \quad (0.3)$$

where $\frac{\sigma_d^2}{\sigma_n^2}$ is the SNR. Once the weights are obtained, symbols are decoded using

$$\hat{a}_j = Q(\bar{w}_j^T \bar{r}^{(1)}). \quad (0.4)$$

\hat{a}_j is the estimate of the bits from j^{th} transmit antenna. $Q(\)$ represents the quantization or slicing operation. After detection, the effect of these symbols is cancelled from the received signal to obtain a modified received signal for next layer of processing. The cancellation is done using

$$\bar{r}^{(2)} = \bar{r}^{(1)} - \hat{a}_j (H)_j, \quad (0.5)$$

where, $(H)_j$ is the j^{th} column of H . (as the subtraction is done after slicing this is hard cancellation). In the next layer, symbols from an other transmit antenna are decoded and cancelled from $r^{(2)}$ in a similar manner as presented above. This process is repeated until symbols from all transmit antennas are decoded. The order in which symbols from each transmit antenna are detected and cancelled, also has an important effect on performance. It was shown in [Wol98] that decoding the signals from the transmit antenna whose SNR at a particular stage is highest among all available antennas and canceling it gives best possible results.

4.1.1 Effect of error propagation in BLAST

Combining array processing and cancellation allows the BLAST receiver to distinguish between signals from various transmit antennas even though no explicit orthogonality is introduced. However, the performance of the BLAST system is limited by accuracy of the symbols detected in the first stage. For this stage the n_R receive antennas should suppress signals from $n_T - 1$ transmit antennas and detect the signals from one antenna. This is equivalent to a system with one transmit antenna and $n_R - n_T + 1$ receive antennas

(Proof is given in *Theorem 1* of [Tar99b]). As the detected symbols are cancelled at each stage, the available diversity increases but any errors made in decisions of the first stage are propagated to later stages. This is called the error propagation problem in BLAST. The inferior power efficiency of BLAST systems is exacerbated by this problem.

The effect of error propagation on BLAST is shown in Figure 4.1.2. Here the BER performance of individual layers of a 8Tx – 8Rx (8X8) BLAST system is compared with (Fig. 4.1.2(b)) and without (Fig. 4.1.2(a)) error propagation. The Zero Forcing algorithm which was described earlier is employed with QPSK symbols. To model the no error propagation case, the receiver is assumed to have exact knowledge of the symbols it is going to cancel at a particular stage. Plots show that due to error propagation, the

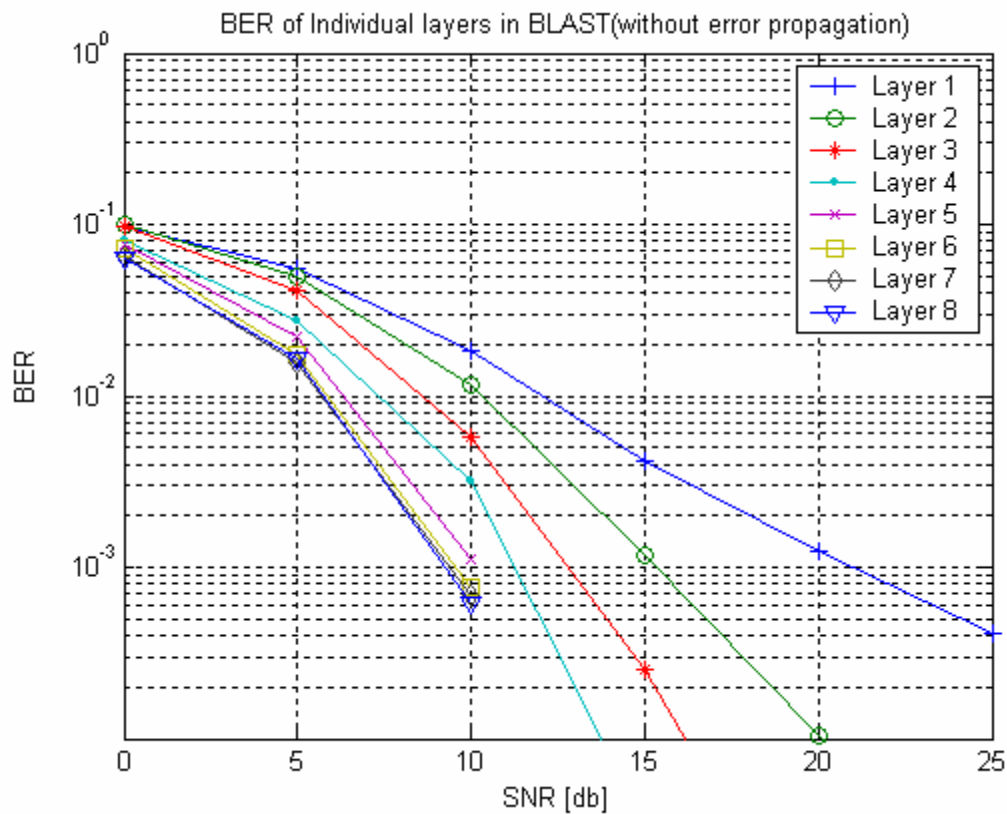


Figure 4.1.2(a) BER of Individual BLAST layers without error propagation (8Tx – 8Rx)

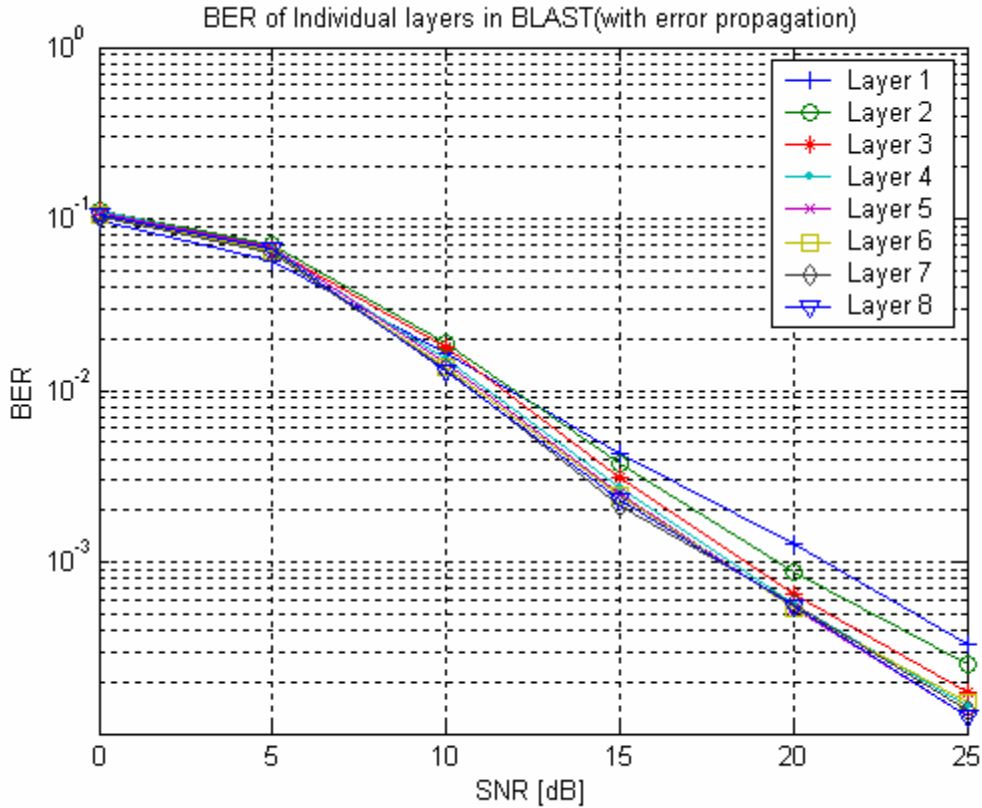


Figure 4.1.2(b) BER of Individual BLAST layers with error propagation (8Tx – 8Rx)

advantage of higher diversity order obtained by cancellation is not fully realized.

Figure 4.1.3 shows the average bit error rate of all the layers of the same 8X8 BLAST system. It can be seen that there is a considerable degradation in the overall performance due to error propagation. However it can also be seen that the effect of error propagation can be considerably reduced by minimizing the decoding errors made in the first stage. This can be expected because, in the 8Tx – 8Rx scenario, the first layer of detection has no spatial diversity advantage (the diversity order is equivalent to a 1Tx – 1Rx system) and thus contributes to a large number of erroneous symbols. If the performance of this layer is improved then the number of errors made in decoding symbols of further layers becomes very low as they get to enjoy a higher diversity advantage.

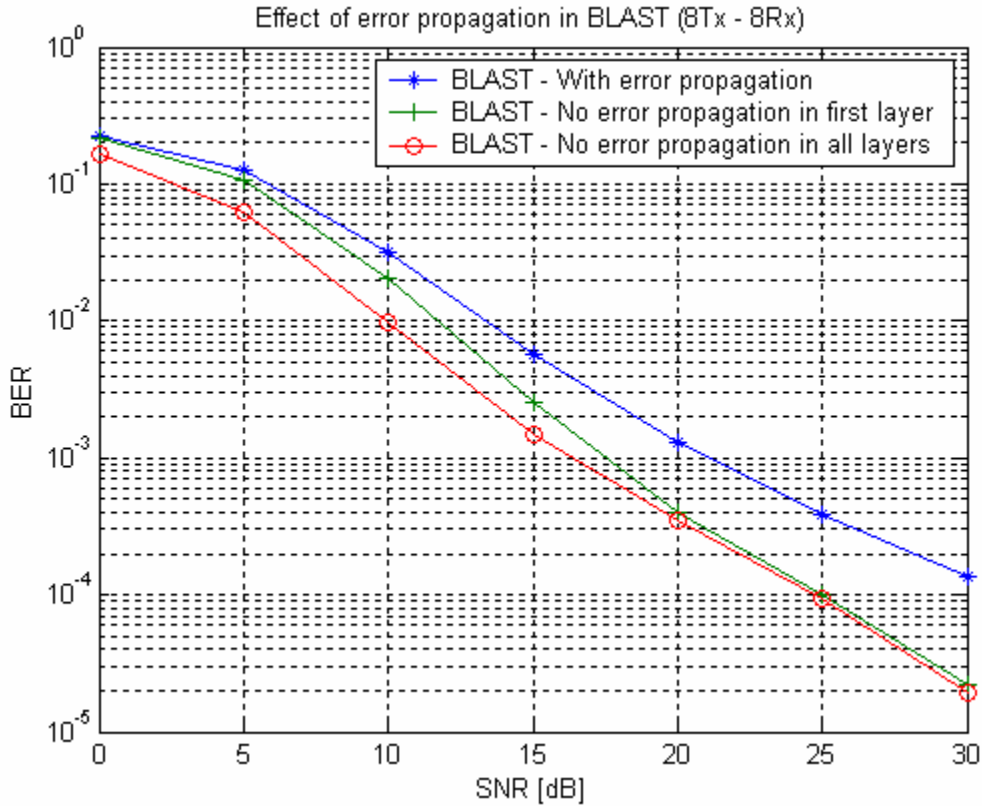


Figure 4.1.3 Effect of error propagation on BLAST (8Tx – 8Rx)

4.1.2 Performance of BLAST in correlated fading

In previous sections the performance of BLAST was characterized for uncorrelated Rayleigh fading channels. However in real environments some correlation between antenna elements can be present. In this section the robustness of layered space-time schemes like BLAST is studied in the presence of correlated fading.

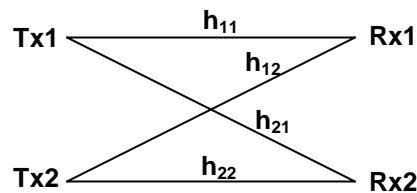


Figure 4.1.4 A 2X2 MIMO channel

Consider a 2X2 MIMO channel shown in Figure 4.1.4. h_{ij} represents the effect of the channel on all signals transmitted from antenna j of the transmitter and received at antenna i of the receiver (hereafter h_{ij} would be called as path gain for convenience of notation). In the 2X2 channel, the paths gains h_{11} and h_{12} (or h_{21} and h_{22}) are from different transmit antennas to a particular receive antenna, so the correlation between these gains can be called transmit correlation ρ_{Tx} . Similarly the paths gains h_{11} and h_{21} (or h_{12} and h_{22}) are those from a particular transmit antenna to different receive antennas and the correlation between these can be called receive correlation ρ_{Rx} . Apart from transmit and receive there can be a correlation between h_{11} and h_{22} (direct-path correlation ρ_D) or between h_{12} and h_{21} (cross-path correlation ρ_{Cr}).

The effect of transmit correlation on BLAST performance is shown in Figure 4.1.5. Here a 4X4 BLAST scheme is used; hence 16 different paths¹ connecting each transmit and receive antenna element are present. Information about the correlation between signals on each path with signals on other paths can be obtained from covariance matrices shown in Figures 4.1.5(b – e). Each block in the covariance matrix plot represents the magnitude of correlation between a particular pair of paths. The structure of the covariance matrix is similar to the one presented in section 3.2 with additional entries added to account for all the 16X16 path pair correlations. The covariance matrix of a spatially uncorrelated channel is shown in Figure 4.1.5(b). Figures 4.1.5(c-e) show covariance matrices of different channels where signals from various transmit paths are correlated and all other possible correlations are nearly zero. The BER plots in Figure 4.1.5(a) show that the performance of BLAST degrades in the presence of transmit correlation. The degradation is mainly due to the noise enhancement caused by the MMSE array processing algorithm.

Performance of MMSE-BLAST in the presence of receive correlation is shown in Figure 4.1.6. The covariance matrices employed to model the necessary receive correlations are

¹ Here ‘path’ means the channel between a particular transmit receive antenna pair.

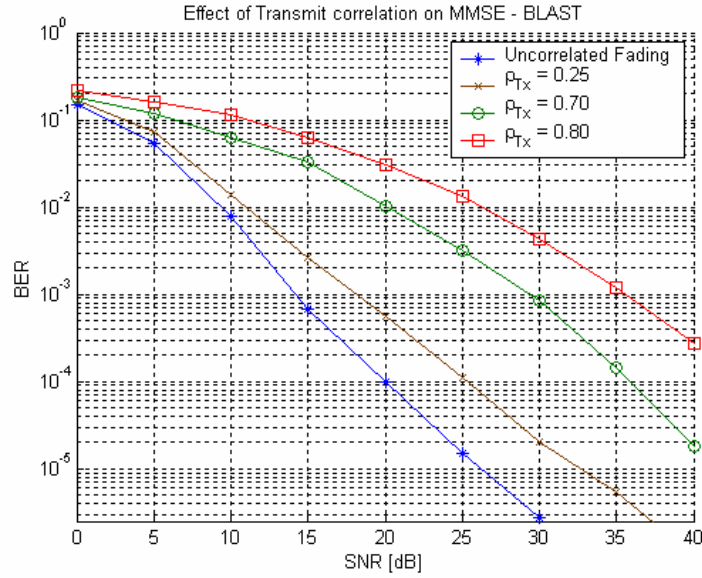


Figure 4.1.5(a) Performance of BLAST with MMSE suppression in the presence of only transmit correlation.

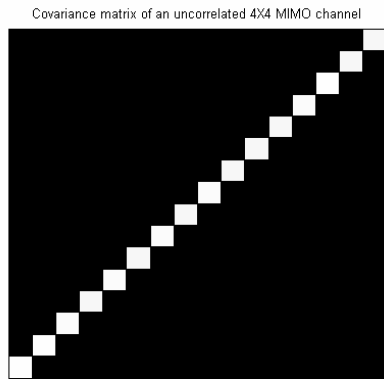


Figure 4.1.5(b)

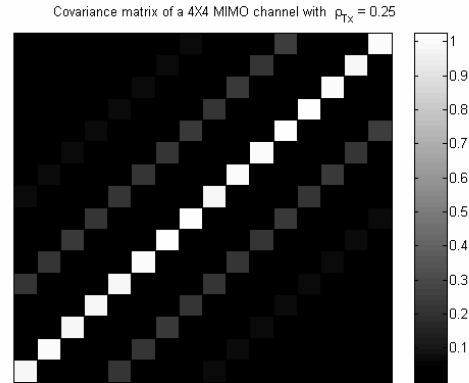


Figure 4.1.5(c)

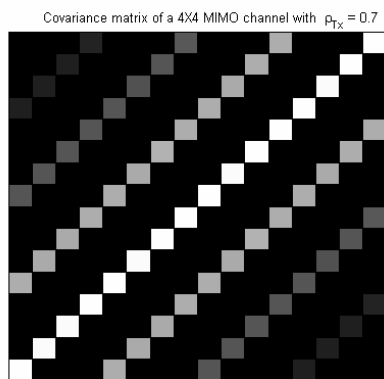


Figure 4.1.5(d)

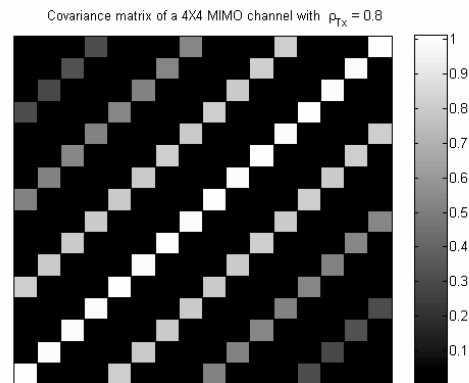


Figure 4.1.5(e)

Figure 4.1.5 (b-e) Covariance matrices of 4X4 MIMO channel model with only transmit correlation. For (b) $|\rho_{Tx}| = 0.0$; for (c) $|\rho_{Tx}| = 0.25$; for (d) $|\rho_{Tx}| = 0.70$; for (e) $|\rho_{Tx}| = 0.80$. Correlation between all other paths is less than 0.1

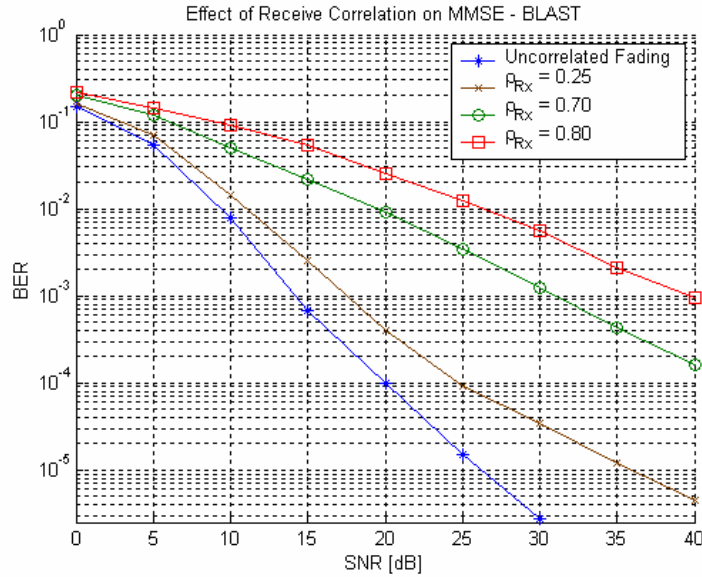


Figure 4.1.6(a) Performance of BLAST with MMSE suppression in the presence of only receive correlation.

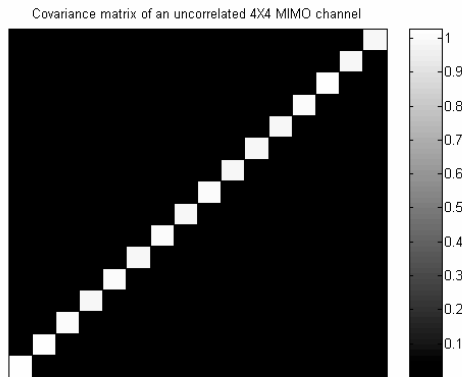


Figure 4.1.6(b)

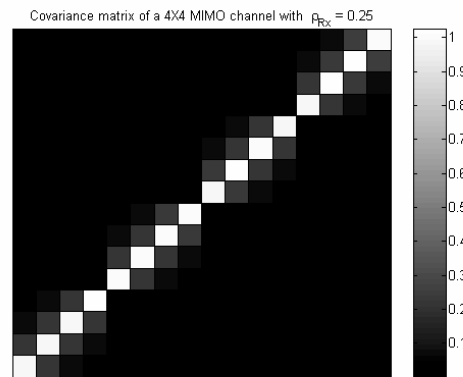


Figure 4.1.6(c)

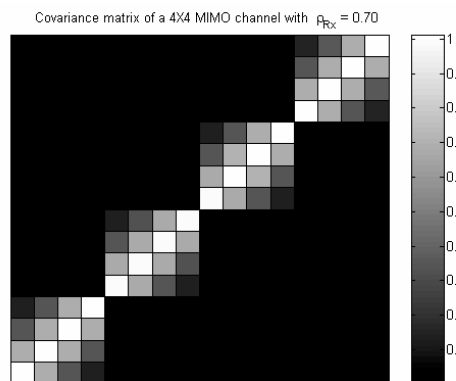


Figure 4.1.6(d)

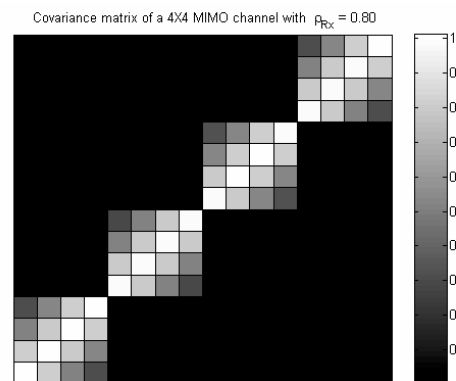


Figure 4.1.6(e)

Figure 4.1.6 (b-e) Covariance matrices of 4X4 MIMO channel model with only receive correlation. For (b) $|\rho_{Rx}| = 0.0$; for (c) $|\rho_{Rx}| = 0.25$; for (d) $|\rho_{Rx}| = 0.70$; for (e) $|\rho_{Rx}| = 0.80$. Correlation between all other paths is less than 0.1

given in figures 4.1.6 (b-e). BER plots in Figure 4.1.6(a) illustrate the degradation for various values of correlation between signals at receive antennas.

Figure. 4.1.7 compares the degradation caused due to receive correlation with the degradation caused by transmit correlation. It can be seen from the figure that the slope of BER curves decreases when received signals are correlated. This indicates a loss in diversity. On the other hand when the transmit signals are correlated the diversity is maintained (slope of transmit correlated BER curves is the same as that of uncorrelated case at higher SNRs) but the performance degrades due to the noise enhancement caused by the MMSE suppression algorithm.

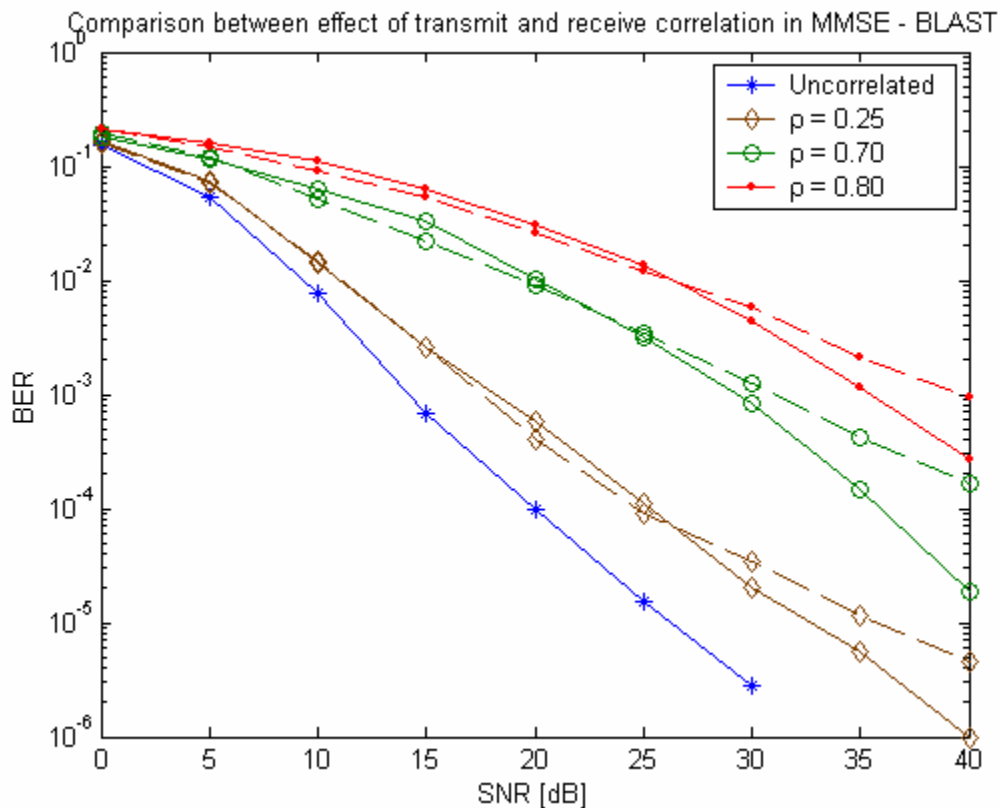


Figure 4.1.7 Comparison between the effect of transmit and receive correlation in MMSE-BLAST. Dotted lines show the BER in the presence of receive correlation while bold lines represent the performance in the presence of transmit correlation.

In channels used to obtain Figure 4.1.5 and Figure 4.1.6, only the transmit or receive correlations were assumed to be present. The correlations between other path pairs, for

instance the direct-path and cross-path, were modeled to be nearly zero (less than 0.1). However in realistic scenarios these correlations may be present. In fact, results from the previous chapter on GBSB-MIMO channels show that for a 2X2 MIMO system a significant amount of direct-path correlation and cross-path correlation can exist even when the transmit and receive correlations are not very high (Figures 3.2.3 and 3.3.6).

Two different channels are considered to study the performance of BLAST in such generic scenarios. In these channels, apart from the transmit and receive correlations, all other possible correlations are also present. The magnitudes of all elements in the covariance matrices of both the channels are shown in Figures 4.1.8(a) and 4.1.8(b). For Channel A the maximum amount of correlation between any two paths ρ_{\max} is limited to 0.3, while for Channel B $\rho_{\max} = 0.4$.

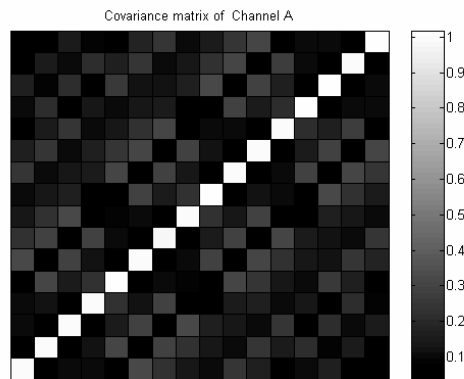


Figure 4.1.8(a)

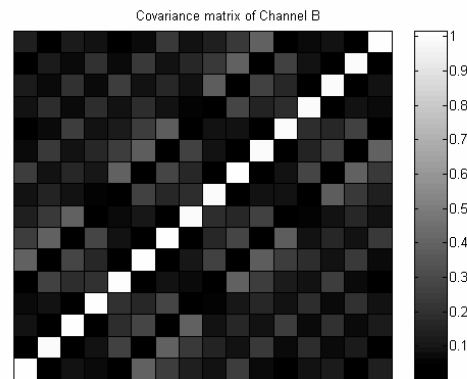


Figure 4.1.8(b)

Figure 4.1.8 (a & b) Covariance matrices of 4X4 GBSB-MIMO channel models. For Channel A shown in 4.1.8(a) $\rho_{\max} = 0.3$. For Channel B shown in 4.1.8(b) $\rho_{\max} = 0.4$

Figure 4.1.8(c) shows the performance of MMSE-BLAST in these channels. Plots indicate degradation of performance in presence of such generalized correlations even when the amount of correlation between any two paths is reasonably low. The degradation in performance can be attributed to the sensitivity of the MMSE suppression algorithm to rank and conditioning of the channel matrix. When the correlation between various paths in the channel increases, the condition number of the channel matrix

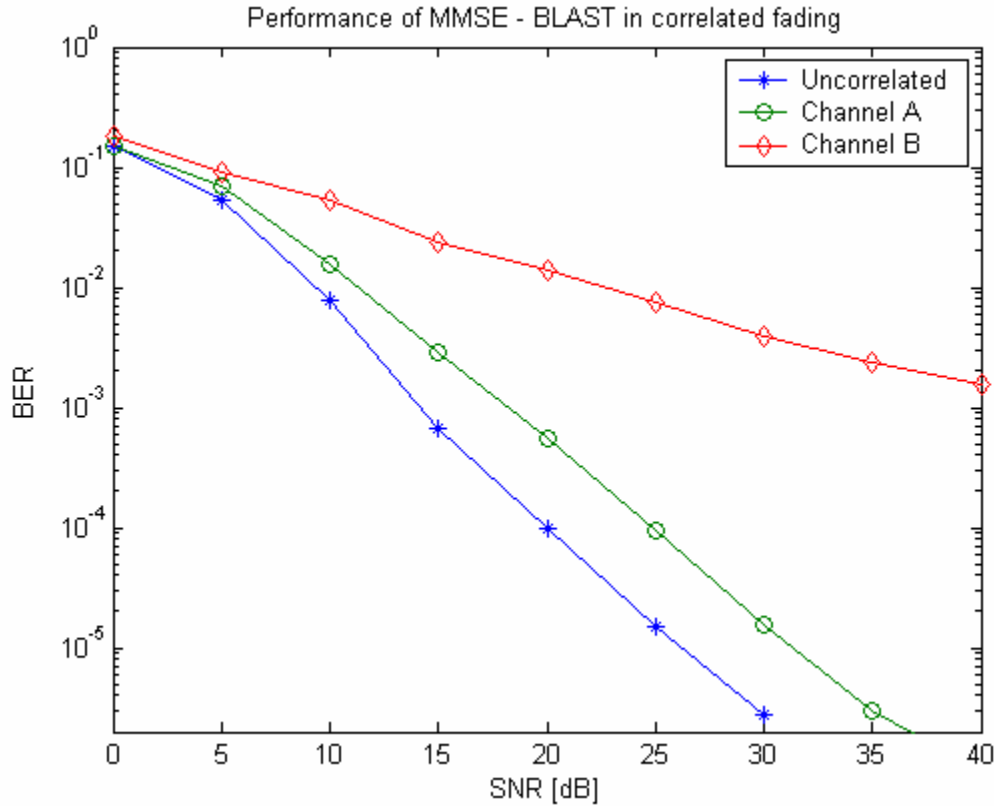


Figure 4.1.8(c) Performance of MMSE-BLAST in general correlated channels. (Other correlations in addition to transmit and receive correlations are also considered in these channels)

(denoted by κ) also increases. κ is the ratio between the largest singular value and the smallest singular value of a matrix. As the matrix becomes ‘more singular’ (elements in the matrix become more correlated) κ approaches infinity. The distribution of κ for Channel A and Channel B is shown in Figure 4.1.9. In this plot the distribution of κ' which is given by $\kappa' = 10\log_{10}(\kappa)$ is plotted as variation in the magnitude of κ is large

Plots show that for Channel B the probability of κ being large is much higher when compared to Channel A. In fact, the distribution of κ for Channel A is close to that of uncorrelated scenario. As noted earlier the noise enhancement of MMSE algorithms increases when κ is large [Bat01]², this degrades the performance of overall BLAST

² The authors in this paper use the reciprocal condition number κ^{-1} in their discussion.

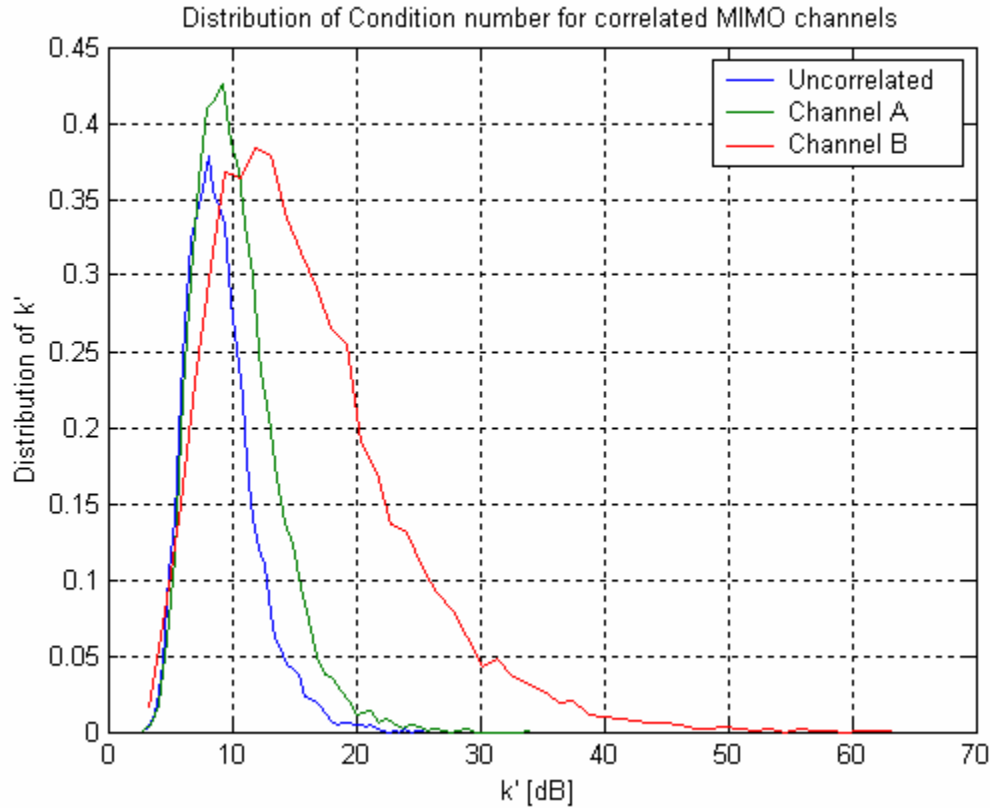


Figure 4.1.9 Distribution of the condition number (in dB scale) for the channel matrices representing Channel A and Channel B.

scheme. The effect of degradation is evident from the corresponding BER curves for each channel in Figure 4.1.8.

4.2 Multilayered Space-Time Coding

This scheme was first proposed in [Tar99b]. Here, the available transmit antennas are partitioned into small groups. Information symbols are transmitted over these groups of antennas by using a separate space-time code for each group. At the receiver, symbols from a particular group of antennas are decoded by suppressing symbols from all other groups by using an array processing algorithm called ‘group interference suppression’. Then, an iterative procedure similar to BLAST is used where symbols decoded from a particular group are cancelled from the received signal before decoding symbols from

other groups. The exact procedure for multilayered space-time coding is explained in the following paragraphs.

Consider a MIMO system with n_T transmit and n_R receive antennas. The channel matrix assuming quasi-static flat fading over each frame of transmitted symbols is represented as

$$H = \begin{bmatrix} h_{1,1} & h_{1,2} & \cdots & h_{1,n_T} \\ h_{2,1} & h_{2,2} & \cdots & h_{2,n_T} \\ \vdots & \vdots & \ddots & \vdots \\ h_{n_R,1} & h_{n_R,2} & \cdots & h_{n_R,n_T} \end{bmatrix} \quad (0.6)$$

where $h_{i,j}$ is the path gain between the i^{th} receive antenna and the j^{th} transmit antenna. Similar to the discussion in Chapter 2 the path gains $h_{i,j}$ are modeled as samples of complex Gaussian random variables with zero mean and unit variance per complex dimension. If the input symbols at any given time are

$$\bar{c} = (c^1 \quad c^2 \quad \cdots \quad c^{n_T})^T \quad (0.7)$$

Then the received signals can be represented using

$$\bar{r}^{(1)} = H\bar{c} + \bar{\eta} \quad (0.8)$$

where, $\bar{r}^{(1)}$ is the $n_R \times 1$ vector of received symbols and $\bar{\eta}$ is a $n_R \times 1$ noise vector of independent AWGN samples. The n_T transmit antennas are partitioned into K groups g_1, g_2, \cdots, g_K with each group having $n_T^1, n_T^2, \cdots, n_T^K$ antennas respectively. It should be noted that $n_T^1 + n_T^2 + \cdots + n_T^K = n_T$. Over each group of n_T^k ($k=1, \dots, K$) antennas a separate space-time code called ‘component code’ C_k is employed for transmitting the symbols. Thus the vector of transmitted symbols \bar{c} can be partitioned

according to the groups into $\bar{c}_1, \bar{c}_2, \dots, \bar{c}_K$ with $\bar{c}_k = (c_k^1 \ c_k^2 \ \dots \ c_k^{n_T^k})^T$ being a $n_T^k \times 1$ vector.

To decode symbols from a specific group, say g_1 , the receiver needs to suppress the symbols from all other groups. It is assumed that the number of receive antennas $n_R \geq n_T - n_T^1 + 1$ and also that the receiver has perfect knowledge about the channel matrix H . Then, H is partitioned into two sub matrices one with dimensions $n_R \times (n_T - n_T^1)$ denoted by

$$\Lambda(g_1) = \begin{bmatrix} h_{1,n_T^1+1} & h_{1,n_T^1+2} & \dots & h_{1,n_T} \\ h_{2,n_T^1+1} & h_{2,n_T^1+2} & \dots & h_{2,n_T} \\ \vdots & \vdots & \ddots & \vdots \\ h_{n_R,n_T^1+1} & h_{n_R,n_T^1+2} & \dots & h_{n_R,n_T} \end{bmatrix} \quad (0.9)$$

and the other with dimensions $n_R \times n_T^1$ denoted by

$$\Omega(g_1) = \begin{bmatrix} h_{1,1} & h_{1,2} & \dots & h_{1,n_T^1} \\ h_{2,1} & h_{2,2} & \dots & h_{2,n_T^1} \\ \vdots & \vdots & \ddots & \vdots \\ h_{n_R,1} & h_{n_R,2} & \dots & h_{n_R,n_T^1} \end{bmatrix}. \quad (0.10)$$

The receiver computes a $(n_R - (n_T - n_T^1)) \times n_R$ matrix $\Theta(g_1)$ [Tar99] such that $\Theta(g_1)\Lambda(g_1) = \mathbf{0}$ ($\mathbf{0}$ is an all zero matrix). $\Theta(g_1)$ is multiplied with the received signal to obtain

$$\tilde{r}^{(1)} = \tilde{\Omega}(g_1)\bar{c}_1 + \tilde{\eta}, \quad (0.11)$$

where,

$$\tilde{\Omega}(g_1) = \Theta(g_1)\Omega(g_1) \quad (0.12)$$

$$\tilde{\eta} = \Theta(g_1)\bar{\eta} \quad (0.13)$$

and $\tilde{r}^{(1)}$ is the $n_R \times 1$ modified received signal vector in which signals from all other groups except g_1 are suppressed. Information symbols transmitted in g_1 are recovered from $\tilde{r}^{(1)}$ by using the decoding algorithm for the corresponding space - time code C_1 . However while decoding, $\tilde{\Omega}(g_1)$ should be employed in place of the channel matrix H . The probability of decoding error for symbols transmitted in group g_1 using this method would be the same as the probability of error obtained by using the space-time code C_1 over a system with n_T^1 transmit antennas and $n_R - (n_T - n_T^1)$ receive antennas (For proof see *Theorem 1* [Tar99b]).

Once the symbols from g_1 are decoded their effect is cancelled from $\bar{r}^{(1)}$ to obtain the received signal vector for the next stage of processing $\bar{r}^{(2)}$. The cancellation should be done by considering the specific signal structure associated with the underlying space-time code. $\bar{r}^{(2)}$ has signals from all the transmit antennas except those belonging to g_1 . Symbols from the next group of antennas are decoded in the same manner as described above. This process is repeated until symbols from all groups are decoded.

It should be noted that BLAST can be considered as a special case of multilayered space-time coding with all groups having a single antenna. Similar to BLAST, as the receiver processing progresses from stage to stage the number of transmit antennas whose signals need to be suppressed is reduced due to iterative cancellation and thus the available diversity order is increased. The BER performance of multilayered space-time coding would be better than that of BLAST because the apart from receive diversity, symbols transmitted from each group also utilize transmit diversity.

The performance of multilayered space-time coding for a 4Tx – 4Rx MIMO system is compared with that of BLAST in Figure 4.2.1.

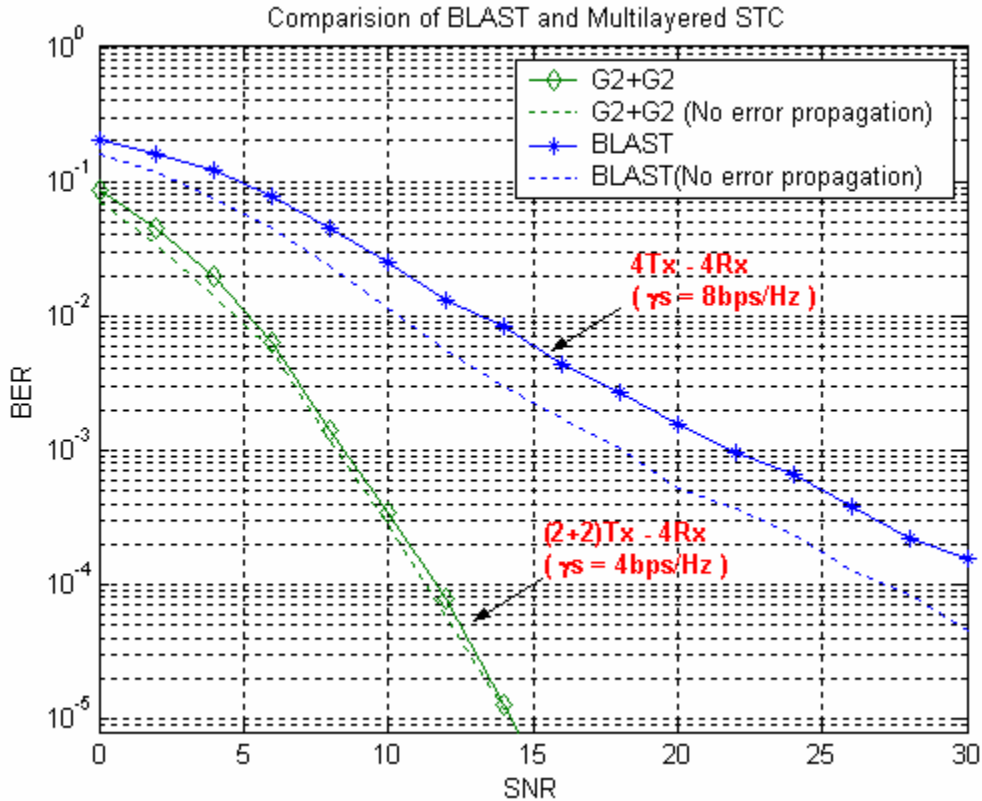


Figure 4.2.1 Comparison of BLAST and Multilayered STC with Space-Time Block codes over each group.

Here, the transmit antennas are partitioned into groups of two each. G2 – STBC is used on each group and QPSK symbols are used for transmission. Symbols of one group are transmitted with two thirds of the total available power while symbols from the other group are transmitted with one third of the total available power. Symbols transmitted from the group with higher power are decoded first.

The spectral efficiency of this scheme is 4bps/Hz. (2bps/Hz each for the two component codes) while that of BLAST is 8bps/Hz. It is clear from the slopes of performance plots that the diversity order obtained by using multilayered space-time coding is much higher than BLAST. This is because, the error performance of the first stage of this multilayered-scheme is equivalent to that of a 2Tx – 2Rx system with G2 – STBC scheme over the transmit antennas and the error performance of the second stage is equivalent to that of 2Tx – 4Rx system with G2 – STBC. Plots also show that the effect of error propagation in the multilayered scheme is minimal. The additional complexity

required at the receiver to implement this scheme is limited to ML detection preceded by a few linear operations.

4.3 Combining STBC and BLAST

Both BLAST and space-time block codes make use of spatial diversity provided by the multiple transmit-receive paths in a MIMO channel. However they utilize it to obtain different kinds of performance benefits over the SISO channel which has no spatial diversity. The BLAST scheme tries to maximize spectral efficiency of the overall system as much as possible while space-time block codes try to improve the signal quality at the receiver (better error performance at low SNR). A good comparison between schemes employing layered decoding (BLAST) and schemes using Space-Time encoding is given in [Bev99].

The encoder for space-time block codes maintains orthogonality among symbols from various transmit antennas. This allows even a single element receiver to distinguish between the signals on different paths. On the other hand, no such encoding is done at the BLAST transmitter to ensure orthogonality, here signals from various transmit antennas are distinguished using array processing with multi-element receivers. This allows the BLAST scheme to achieve very high spectral efficiency as its encoder does not add any redundancy in both the space and time domains. However the power efficiency of BLAST is very low since its performance is limited by errors made in the first layer of processing which has the lowest diversity order.

The multilayered space-time coding scheme discussed in the previous section uses transmit diversity in the form of space-time block codes to decrease the decoding errors in individual layers, but using space-time block codes over all groups reduces the spectral efficiency of the transmission scheme. Plots in Figure 4.1.3 show that the performance of layered detection algorithm in BLAST can be significantly improved if the errors made in first layer are reduced. Therefore, space-time block codes can be used to improve the

error performance of the first layer of detection and symbols on other layers can be transmitted by encoding without any redundancy.

For example in a 4Tx – 4Rx scenario, symbols on two antennas can be encoded using space-time block codes while the symbols on other two antennas can be transmitted in a BLAST like manner without any redundancy. Such a coding scheme can be called G2+1+1. The structure of this scheme would be

$$G2+1+1 = \begin{pmatrix} x_1 & x_2 & x_3 & x_4 \\ -x_2^* & x_1^* & x_5 & x_6 \end{pmatrix}. \quad (0.14)$$

6 symbols are transmitted here in two time intervals, so the spectral efficiency of the scheme with M-ary PSK modulation would be $3M$ bps/Hz. The spectral efficiency of this scheme is slightly less than BLAST ($4M$ bps/Hz) but a significant gain can be obtained in terms of power efficiency. Alternate schemes like

$$G2+G2 = \begin{pmatrix} x_1 & x_2 & x_3 & x_4 \\ -x_2^* & x_1^* & -x_4^* & x_3^* \end{pmatrix} \quad (0.15)$$

$$G3+1 = \begin{pmatrix} x_1 & x_2 & x_3 & x_5 \\ -x_2 & x_1 & -x_4 & x_6 \\ -x_3 & x_4 & x_1 & x_7 \\ -x_4 & -x_3 & x_2 & x_8 \\ x_1^* & x_2^* & x_3^* & x_9 \\ -x_2^* & x_1^* & -x_4^* & x_{10} \\ -x_3^* & x_4^* & x_1^* & x_{11} \\ -x_4^* & -x_3^* & x_2^* & x_{12} \end{pmatrix} \quad (0.16)$$

which have lower spectral efficiencies ($2M$ bps/Hz for G2+G2, $1.5M$ bps/Hz for G3+1) but better power efficiency, can also be employed. The performance of these schemes in an uncorrelated Rayleigh fading channel is compared with the V-BLAST scheme (which

has the best spectral efficiency) and the G4 scheme (which has the best power efficiency) in Figure 4.3.1. QPSK modulation is used for transmission.

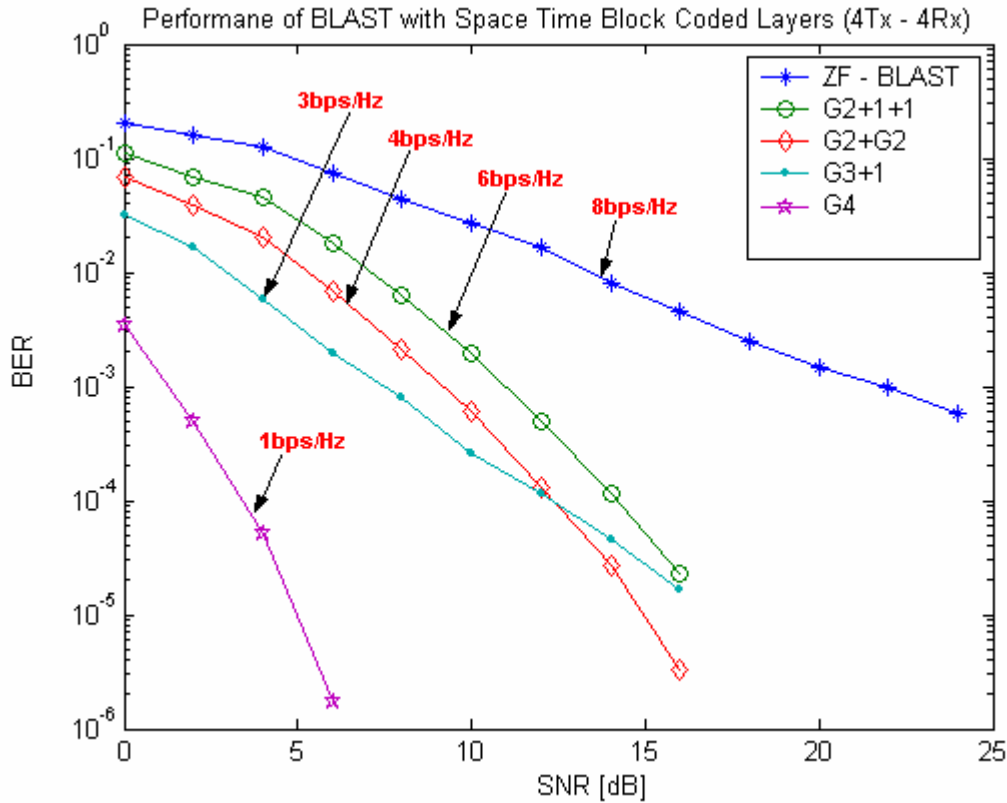


Figure 4.3.1 Performance of BLAST with STBC layers (4Tx – 4Rx, QPSK)

Plots clearly illustrate the trade-off between spectral efficiency and power efficiency. In fact the G2+1+1 scheme is about 11dB better than BLAST at a BER of 10^{-3} with only a little penalty in spectral efficiency. This is because in G2+1+1, the first layer gets a diversity advantage equivalent to a 2Tx-2Rx system and even the second layer has a diversity advantage equivalent to a 1Tx– 3Rx system which is better than that of BLAST second layer whose diversity advantage is equivalent to a 1Tx – 2Rx system.

Another advantage of partitioning a few transmit antennas into groups is that the number of receive antennas in the MIMO system can be less than the number of transmit antennas. The number of receive antennas can be as low as $n_{R_{\min}} = n_T - (n_T^{\max} - 1)$ where

$n_T^{s_{\max}}$ is the maximum number of antennas in any particular group. Having more than $n_{R_{\min}}$ receive antennas helps the interference suppression algorithms like ZF and MMSE in distinguishing between signals from various transmit antennas.

The robustness of BLAST with space-time block coded layers to correlation is shown in figure 4.3.2. The GBSB-MIMO model used in the previous section called Channel B, where correlations between any two paths are less than 0.4, is employed here to model the required correlated fading.

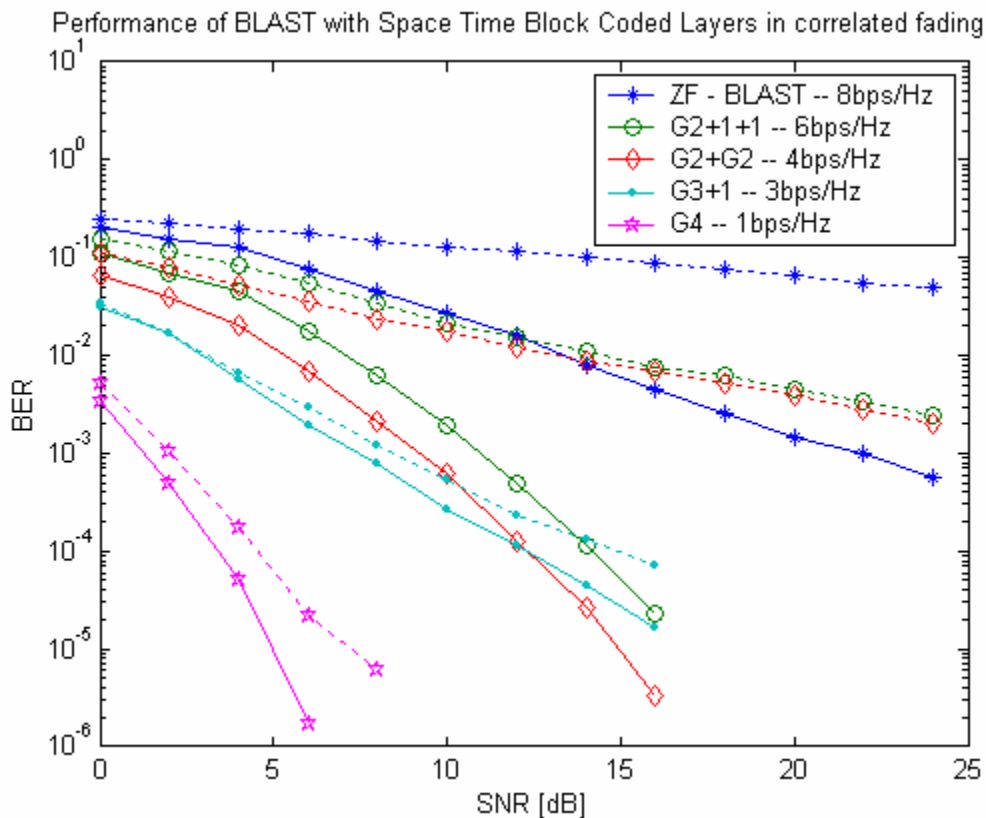


Figure 4.3.1 Performance of BLAST with STBC layers (4Tx – 4Rx, QPSK) in correlated fading. (Bold lines show the performance in uncorrelated channel; dotted lines show the performance in correlated channels).

Performance curves clearly illustrate that BLAST, $G2+1+1$, $G2+G2$ are very sensitive to correlation as they rely on interference suppression at the receiver for distinguishing between signals from various transmit antennas. It can also be seen from the plots that the

robustness of receiver processing in presence of correlation improves as more and more orthogonality is introduced at the transmitter.

4.4 Transmit Beamforming and Space-Time Coding

Space-Time block coding schemes are designed for scenarios where the transmitter does not have any information about the downlink channel. However in certain systems, the transmitter may have some channel information. For example, the WCDMA standard provides a mode of operation where the receiver estimates the downlink channel and sends this information to the transmitter on a reverse feed back loop [3GP01]. In such situations the available channel state information can be used to improve performance. This section presents a brief discussion of the various issues involved in combining transmit beamforming and space-time block coding.

In receive antenna array literature, when the signal arrives at all the elements of a particular array from a single direction the array is usually called as a ‘directive array’. Here the effect of the channel on all array elements is the same. On the other hand, when the received signal has no particular direction of arrival, which means that the effect of the channel at each element of the array is different, the array is called a ‘diversity array’. It should be noted that the notion that a particular array is called a ‘directive array’ or a ‘diversity array’ depends on how the channel affects the signals at each element of the array. It is also important to note that in both cases optimum reception is obtained by undoing the distortion of the channel. i.e., if the channel is represented by a vector of complex numbers with each element representing the distortion at a particular antenna element, then multiplying signal at each receive element by the conjugate of its corresponding channel coefficient and adding these modified signals is the optimum way of reception. In fact in both cases of directive and diversity arrays, this processing amounts to spatial filtering to collect energy from some directions and ignore energy from other directions. In the case of directive arrays it is straightforward to visualize this process, but for diversity arrays this fact is less apparent, as it is difficult to determine a particular direction of arrival.

A similar discussion is valid for transmit arrays too. So, the term ‘transmit beamforming’ can be understood as the process of focusing the transmit energy towards the location of the receiver by using array processing. The best way of doing this is multiplying the transmit signal at each transmit array element by the conjugate of its corresponding channel coefficient, whatever the value of correlation between the channel coefficients might be. With this notation, ‘transmit beamforming’ in the directive array sense, in fact becomes a special case where all the channel coefficients are perfectly correlated. Basic principles of transmit beamforming where the down link channel information is obtained via feed-back from the transmitter are explained in [Ger94].

Information theoretic results [Ara99] show that for a MISO channel (multiple transmit antennas and a single receive antenna), transmit beamforming is the optimum way of maximizing both SNR and the amount of information reaching the receiver from the transmitter (measured in terms of mutual information³) provided that exact information about the downlink channel is available. If the channel is represented by

$$\bar{h} = [h_1 \quad h_2 \quad \cdots \quad h_{n_r}]^T, \quad (0.17)$$

and the data symbol to be transmitted is c .

(0.18)

Then transmitting,

$$\bar{X} = \frac{\bar{h}^*}{\|\bar{h}\|} c \quad (0.19)$$

maximizes the mutual information and also the SNR at the receiver[Ara98]. Note that (4.19) is transmit beamforming towards the location of the receiver in a direction indicated by the channel coefficients.

³ This is the reduction in uncertainty of one random variable due to the knowledge of other (see pp 18 in [Cov91]). By modeling both the transmitted and received symbols as random variables the amount of information conveyed by the transmitter symbols in determining the received symbols can be measured in terms of mutual information.

As the quality of channel information at the transmitter degrades, employing beamforming may not always be optimal [Ara98]. In fact when no information about the channel is available, the best possible strategy at the transmitter would be radiating equally in all directions. In such cases, using vector coding schemes (for example space-time codes) where different information symbols are transmitted from various transmit elements, should be used to maximize the mutual information. On the other hand, when vector coding is used, the available power for each transmitted symbol is reduced by a factor n_t as the total transmit power is a constant. Due to this each transmitted symbol is received with a lower average power when compared to beamforming. Therefore, in order to optimize performance the transmitter needs to choose either beamforming or vector coding depending on the accuracy of the channel estimates and the signal to noise ratio (SNR).

A scheme where the transmitter switches between beamforming and space-time block coding in a spatially uncorrelated Rayleigh fading channel was proposed in [Jon02]. Here when the information about the channel is reliable, the transmitter performs beamforming and when the channel estimates become noisy the transmitter antennas use space-time block codes and radiate isotropically in all directions. The parameter which decides when this switching is done depends on various factors which include; the type of space-time block code used, instantaneous SNR, number of transmit antennas and also the correlation ρ_c between the noisy channel estimates and true estimates. Some of these parameters are predefined while others need to be estimated at the receiver.

Results for the scheme in [Jon02] indicate that at low SNR values, employing beamforming gives better performance in terms of bit error rate of received symbols when compared to schemes using space-time block codes, provided that the channel estimates are good. At higher SNR values the BER performance obtained by using beamforming is either worse or same as that of space-time block codes. As the accuracy of channel estimates degrades, the SNR values where beamforming has the advantage over space-time block coding become lower. Results also reaffirm that, if perfect channel

estimates are available, using transmit beamforming always gives better performance than space-time block coding.

4.5 Summary

In this chapter, a detailed analysis of schemes which use space-time coded modulation at the transmitter and array processing at the receiver was provided. Performance results indicate that these schemes can provide reliable high data rate wireless communication at reasonable values of signal to noise ratio. Analysis also shows that correlation in MIMO channels can severely degrade performance if the receiver relies on array processing to distinguish between signals from various transmit antennas. Finally, the chapter also provided a brief discussion on various issues involved in combining transmit beamforming and space-time block coding.

Chapter 5

Conclusions

This chapter concludes the thesis by summarizing the work presented so far and providing a few directions for future investigation.

5.1 Summary of Results

The focus of this thesis was on developing GBSB-MIMO channel models and analyzing the performance of STBC and BLAST in these models. A chapter wise summary of the results presented in his thesis is given below.

In Chapter 2, a brief review of the current literature on MIMO channel models was given and various transmit diversity techniques were discussed. Following that, space-time block codes were introduced and their performance was analyzed in uncorrelated quasistatic Rayleigh fading channels.

In Chapter 3, fading correlation between signals at various antenna elements was characterized for GBSB circular and elliptical MIMO channel models. The performance of space-time block codes was then studied for these GBSB-MIMO models. Results show that the correlation between various paths in the channel is dependent on the spacing between antenna elements of the transmit and receive arrays and also on the geometry of distribution of scatterers. Performance plots for STBC indicate a relatively

small degradation of performance for low to medium values of correlation and a loss of diversity order for very high correlation.

In Chapter 4, schemes which use space-time coded modulation at the transmitter and array processing at the receiver were introduced and their performance was analyzed for uncorrelated and correlated MIMO fading scenarios. Results indicate that these schemes can provide reliable high data rate wireless communication at reasonable values of signal to noise ratio. Analysis also shows that correlation in MIMO channels can severely degrade performance if the receiver relies on array processing to distinguish between signals from various transmit antennas.

5.2 Future Work

A few possible extensions to the work presented in this thesis are listed below.

- GBSB-MIMO channel models used in this work assume a flat fading environment. However, in CDMA systems, the signals usually undergo frequency selective fading and various multipath components can be resolved. It would be useful to extend the analysis on GBSB-MIMO models in Chapter 3 to account for frequency selective fading.
- Another possible extension to the MIMO channel models is to use ‘double bounce scattering’ [Moli02a] instead of single bounce scattering. This would allow the models to characterize the ‘keyhole’ or ‘pinhole’ effects which reduce the rank of the channel matrix.
- Schemes which switch between space-time block coding and transmit beam forming on the basis of available channel information were proposed recently in [Jon02]. The analysis of such schemes has been so far restricted to uncorrelated fading. Performance of these schemes in correlated fading can be studied by using the channel models presented in this thesis.

Bibliography

- [3GP01] 3rd Generation partnership project (3GPP) “Physical layer procedures”, report, 3GPP TS 25.214 v4.3.0, release 4, Dec 2001.
- [3GP02] 3rd Generation partnership project (3GPP) “Physical layer channels and mapping of transport channels onto physical channels”, report, 3GPP TS 25.211 v4.3.0, release 4, Dec 2001.
- [Ala98] Siavash. M. Alamouti, “A simple transmit diversity technique for wireless communications”, *IEEE Journal on Selected Areas in Communications*, vol.16, pp. 1451-1458, October 1998.
- [Alex01] Angeliki Alexiou, “Realistic channel model considerations in UMTS downlink capacity with space-time block coding”, *SPAWC' 01*, pp.275-278, March 2001.
- [Ara98] Aradhana Narula, Mitchell J. Lopez, Mitchell D. Trott, Gregory W. Wornell, “Efficient use of side information in multiple antenna data transmission over fading channels”, *IEEE Journal on Selected Areas in Communications*, vol.16, no.8, pp. 1423-1436, October 1998.
- [Ara99] Aradhana Narula, Mitchell D. Trott, Gregory W. Wornell, “Performance limits of coded diversity methods for transmitter antenna arrays”, *IEEE Transactions on Information theory*, vol.45, no.7, pp.2418-2433, November 1999.
- [Bar00] Stephan Baro, Gerard Bauch, Aneta Pavlic, Andreas Semmler, “Improving BLAST performance using Space-Time Block codes and Turbo Decoding”, *IEEE Global Telecommunications Conference, GLOBECOM '00*, vol.2, pp.1067 -1071, 2000.

- [Bat01] M.D. Batarriere, J.F. Kepler, T.P. Krauss, S. Mukhtavaram, J.W. Porter, F.W. Vook, "An experimental OFDM system for Broadband Mobile Communications", *IEEE Vehicular Technology Conference*, vol.4, pp.1947-1951, Fall 2001.
- [Bat02] M.D. Batarriere, T.K. Blankenship, J.F. Kepler, T.P. Krauss, I. Ilicia, S. Mukhtavaram, J.W. Porter, T.A. Thomas, F.W. Vook, "Wideband MIMO impulse response measurements at 3.8GHz", *IEEE Vehicular Technology Conference, Spring 2002*.
- [Bev99] D. Bevan, R. Tanner, "Performance comparison of space-time coding techniques", *IEEE Electronics Letters*, vol.35, no.30, pp.1707-1708, September 1999.
- [Blum02] R.S. Blum, J.W. Winters, "On optimum MIMO with antenna selection", *IEEE International Conference on Communications*, vol.1, pp.386-390, May 2002.
- [Bue00] R.M. Buehrer, "Generalized equations for spatial correlation for low to medium angle spread", *10th Annual Virginia Tech symposium on wireless personal communications*, June 2000.
- [Bue01] R. Michael Buehrer, Sridhar Arunachalam, Kam H. Wu, Andrea Tonello, "Spatial Channel Model and measurements for IMT – 2000 Systems", *IEEE VTC*, Spring 2001, vol.1, pp.342-346.
- [Chiz00a] D. Chizhik, F. Rashid-Farrokhi, J. Ling, A. Lozano, "Effect of antenna separation on the capacity of BLAST in correlated channels", *IEEE Communications Letters*, vol.4, pp.337-339, November 2000.
- [Chiz00b] D. Chizhik, G.J. Foschini, R.A. Valenzuela, "Capacities of multi-element transmit and receive antennas: correlations and keyholes", *IEEE Electronics letters*, vol.36, pp.1099-1100, June 2000.

- [Chiz02] D. Chizhik, G.J. Foschini, M.J. Gans, R.A. Valenzuela, "Keyholes, correlations, and capacities of multielement transmit and receive antennas", *IEEE Transactions on wireless communications*, vol.1, pp.361-368, April 2002.
- [Cov91] T. Cover, J.A. Thomas, *Elements of Information Theory*, Wiley series in telecommunications, 1991.
- [Dur99] G.D. Durgin, T.S. Rappaport, "Effects of multipath angular spread on the spatial correlation of received signal voltage envelopes", *IEEE VTC'99*, pp.996-1000.
- [Ert98a] Richard B. Ertel, "Antenna Array Systems: Propagation and Performance", *PhD. Thesis, Virginia Tech*, July 1999.
- [Ert98b] Richard B. Ertel, Paulo Cardieri, Kevin W. Sowerby, T. S. Rappaport, J. H. Reed, "Overview of Spatial Channel Models for Antenna Array Communication Systems", *IEEE Personal Communications*, vol.5, pp. 10-22, Feb 98.
- [Fos96] G.J. Foschini, "Layered space-time architecture for wireless communication in a fading environment when using multielement antennas", *Bell Labs Technical Journal*, vol.1, no.2, pp. 41-59, Autumn 1996.
- [Fos98] G.J. Foschini, M.J. Gans, "On limits of wireless communication in a fading channel when using multiple antennas", *Wireless Personal Communications*, vol.6, no.3, pp. 311-335, March 1998.
- [Gesb00a] D. Gesbert, H. Bolcskei, D. Gore, A.J. Paulraj, "MIMO wireless channels: Capacity and performance prediction", *IEEE GLOBECOM'00*, vo.2 pp.1083-1088, 2000.

[Gesb00b] D. Gesbert, H. Bolcskei, D. Gore, A.J. Paulraj, “Performance evaluation for scattering MIMO channels”, *34th Asilomar conference on signals systems and computers*, vol.1, pp. 748-752, 2000.

[Ger94] D. Gerlach, A.J. Paulraj, “Adaptive transmitting antenna arrays with feedback”, *IEEE Signal Processing Letters*, vol.1, pp.150-152, October 1994.

[Goz02a] Ran Gozali, Brian D. Woerner, “On Robustness of Space Time Block Codes to Spatial Correlation”, *IEEE VTC*, Spring 2002.

[Goz02b] Ran Gozali, Brian D. Woerner, “Theoretic bounds of orthogonal design transmit diversity over independent and correlated fading channels”, accepted for publication in ISIT’02.

[Goz02c] R. Gozali, R. Mostafa, R.C. Palat, R. Nory, B.D. Woerner, J.H. Reed, “On performance of orthogonal STBC in indoor and outdoor MIMO wireless channels using analysis, simulation and measurement campaign”, *Submitted to IEEE Journal on Selected Areas in Communications*, 2002.

[Hea01a] R.W. Heath Jr., S. Sandhu, A. J. Paulraj, “Antenna selection for spatial multiplexing systems with linear receivers”, *IEEE Communications Letters*, vol.5, pp. 142-144, April 2001.

[Jon02] George Jongren, Mikael Skoglund, Bjorn Ottersten, “Combining beamforming and orthogonal space-time block coding”, *IEEE Transactions on Information theory*, vol.48, no.3, pp.611-627, March 2002.

[Lee73] W.C.Y. Lee, “Effects on correlation between two mobile radio base station antennas”, *IEEE Trans. Communications*, vol.COM-21, pp.1214-1224, November 1973.

[Lib96] Joseph C. Liberti, T. S. Rappaport, “A Geometrically Based Model for Line of Sight Multipath Radio Channels “, *IEEE VTC*, 1996, vol.2, pp. 844-848.

[Lu97] Ming Lu, Titus Lo, John Litva, “ A physical Spatio-Temporal model of multipath propagation channels” , *IEEE VTC 97*, vo.2, pp.810-814.

[Moli02a] A.F. Molisch, “A generic for MIMO wireless propagation channels”, *IEEE International Conference on Communications*, vol. 1, pp.277-282, May 2002.

[Moli02b] A.F. Molisch, “A Channel model for MIMO systems in macro- and microcellular environments”, *IEEE VTC*, Spring 2002.

[Rap96] T. S. Rappaport, “Wireless Communcations, Principles and Practice” , 1996 , Prentice Hall PTR.

[Rens00] C.V. Rensburg, B. Friedlander, “Transmit diversity for arrays for correlated rayleigh fading”, *34th Asilomar conference on signals systems and computers*, vol.1, pp. 301-305, 2000.

[Salz94] J. Salz, J.W. Winters, “Effect of fading correlation on adaptive antenna arrays in digital mobile radio”, *IEEE Transactions on Vehicular Technology*, vol.43, pp. 1049-1057, November 1994.

[Sand01] S. SAndhu, R. Heath, A. Paulraj, “Space-Time block codes versus space-time trellis codes”, *IEEE International conference on communications*, vol.4, pp. 1132-1136, 2001.

[Shiu00] Da-Shan Shiu, G. J. Foschini, M. J. Gans, J. M. Kahn, “Fading correlation and its effect on multielement antenna systems”, *IEEE Trans. Commmun.*, vol.48, pp.502-513, March 2000.

- [Stoy01] M. Stoychev, H. Safar, "Statistics of the MIMO radio channel in indoor environments", *IEEE VTC'01*, vol.3, pp. 1804-1808, Fall 2001.
- [Tar98] V. Tarokh, N. Seshadri, A. R. Calderbank, "Space-Time codes for high data rate wireless communication :Performance criterion and code construction", *IEEE Transactions on Information Theory*, vol.44, pp.744-765, March 1998.
- [Tar99a] V. Tarokh, H. Jafarkhani, A. R. Calderbank, "Space-Time Block Coding for wireless communications: Performance Results", *IEEE Journal on Selected areas in communications*, vol.17, pp.451-460, March 99.
- [Tar99b] Vahid Tarokh, Ayman Naguib, Nambi Seshadri, A.R. Calderbank, "Combining array processing and space-time coding", *IEEE Transactions on Information theory*, vol.45, no.4, pp.1121-1128, May 1999.
- [Ter99c] V. Tarokh, H. Jafarkhani, A. R. Calderbank, "Space-Time Block codes from orthogonal designs" , vol.45, pp.1456-1467, July 1999.
- [Tra92] T. T. Tran, T. S. Rappaport, "Site Specific propagation prediction models for PCS design and installation" , *IEEE MILCOM*, 1993, vol.2, pp. 1062-1065.
- [Win83] J.H. Winters, " Switched diversity for feedback with DPSK mobile radio systems", *IEEE Transactions on Vehicular technology*, vol.VT-32, pp. 134-150, February 1983.
- [Wol98] P.W.Wolniansky, G.J. Foschini, G.D. Golden, R.A. Valenzuela, "V-BLAST: An architecture for realizing very high data rates over the rich scattering wireless channel", *URSI International Symposium on Signals, Systems, and Electronics ISSSE 98*, pp.295-300, 1998.

Vita

Ravikiran Nory was born on February 28, 1979 in the city of Bangalore, India. He received his B.Tech degree in Electronics & Communication engineering from Jawaharlal Nehru Technological University, India in June, 2000. Ravi joined the M.S. program in Electrical Engineering at Virginia Tech in August, 2000 and is currently working as a Graduate Research Assistant at the Mobile and Portable Radio research Group (MPRG) under the guidance of Dr. Brian Woerner. His research interests include propagation, channel modeling and receiver design for wireless communication systems.

In the summer of 2001, Ravi worked as an Engineering Intern with the location group of Motorola PCS Research labs in Libertyville, Illinois. He will be joining the same group as an Engineer in July 2002.